The damaging character of shallow 20th century earthquakes in the Hainaut coal area (Belgium)

Thierry Camelbeeck[1], Koen Van Noten[1], Thomas Lecocq[1], and Marc Hendrickx[1]

[1]Royal Observatory of Belgium, Seismology-Gravimetry. Avenue Circulaire 3, 1180 Uccle, Belgium.

Correspondence: Thierry Camelbeeck (Thierry.Camelbeeck@oma.be)

Abstract. The present study analyses the impact and damage of shallow seismic activity that occurred from the end of the 19th century until the late 20th century in the coal area of the Hainaut province in Belgium. This seismicity is the second largest source of seismic hazard in northwestern Europe, after the Lower Rhine Embayment. During this period, five earthquakes with moment magnitudes (M_W) around 4.0 locally caused widespread moderate damage to buildings corresponding to maximum intensity VII in the EMS-98 scale. Reviewing intensity data from the official macroseismic surveys held by the Royal Observatory of Belgium, press reports, and contemporary scientific studies resulted in a comprehensive macroseismic intensity data set. Based on this data set, we created macroseismic maps for 28 earthquakes, and established a new Hainaut intensity attenuation model and a relationship linking magnitude, epicentral intensity and focal depth. Using these relationships, we estimated the location and magnitude of pre-1985 earthquakes that occurred prior to deployment of the modern digital Belgian seismic network, resulting in a new updated earthquake catalogue for the Hainaut area for this period including 124 events. A comparison with other areas worldwide where currently similar shallow earthquake activity occurs, suggests that intensity attenuation is strong in Hainaut. This high attenuation and our analysis of the cumulative effect of the Hainaut seismicity indicate that current hazard maps overestimate ground motions in the Hainaut area. This reveals the need to use more appropriate ground motion models in hazard issues. Another strong implication for earthquake hazard comes from the reliability of the computed focal depths that helps clarifying the hypotheses about the origin of this seismicity. Some events were very shallow and occurred near the surface up to a depth not exceeding 1 km, suggesting a close link to mining activities. Many events, including the largest shallow events in the coal area before 1970, occurred at depths greater than 2 km, which would exclude a direct relationship with mining, but still might imply a triggering causality. A similar causality can also be questioned for other events that occurred just outside of the coal area since the end of the mining works.

1 Introduction

Moderate shallow earthquakes with magnitudes in the range of 4.0 to 6.0 have a real potential of destruction when they occur in populated areas. This is particularly the case in regions where the building stock is old and vulnerable, and contains few earthquake-resistant buildings. In seismically active regions, even if 4.0 M_W earthquakes can be locally damaging (Nappi et al., 2021), current hazard is associated with the upper part of this magnitude range. In Western Europe, M_W 4.0 to 5.0 shallow earthquakes represent the most probable current source of seismic risks, which is currently enhanced by the increase

of induced seismicity by underground energetic resources (Grigoli et al., 2017; Nievas et al., 2020). In Western Europe, the potential of destruction of shallow earthquakes was exemplified by the damaging impact of the 11 May 2011 Lorca (Spain, M_W=5.1, Association Française de génie Parasismique, 2011), 16 August 2012 Huizinge (The Netherlands, M_W=3.6, Dost and Kraaijpoel, 2013) and the 11 November 2019 Le Teil (France, M_W=4.9, Sira et al., 2019) earthquakes.

30   In southern Belgium, Namurian to Westphalian (Upper Carboniferous) coal seams have been intensively exploited in the 19th and 20th century in *"la bande Houillère"*, i.e. a narrow, 10 to 15 km wide geological region located between the Belgian cities of Mons in the West and Liège in the East (Fig. 1). This coal mining area is bordered in the south by the Midi Fault, which manifests the overthrusting of the Ardenne Allochton (including the Dinant Fault-and-Thrust Belt and High-Ardenne slate belt) over the Brabant Parautochton. In the north, the coal mining area is limited up to the northern occurrence of the

35   Westphalian (Fig. 2), which overlains the Lower Palaeozoic Brabant Massif. Mining in the coal area in the province of Hainaut (further referred to as the Hainaut coal area) was focused on three basins: the Borinage-Mons basin, the Centre-La Louvière Basin and the Charleroi basin. In the Centre-La Louvière and Charleroi basins, the sedimentary cover thickness is minor. In the Borinage-Mons basin, Cretaceous deposits up to 300 m thick cover the Westphalian. While no earthquakes were reported in the Hainaut coal area in the first part of the 19th century during which intense coal mining began, seismicity began in 1887 (Table

40   1, Fig. 2) and continued up to the present. This seismicity is unique in Belgium and neighbouring regions as five events with M_W 4.0 caused locally widespread, moderate to extensive damage to buildings. Before this study, the origin of this earthquake activity was considered as natural.

    The main characteristics of seismic events in the Hainaut coal area are the high epicentral intensity and the rapid intensity decay with distance, suggesting shallow focal depths (Charlier, 1949; Van Gils, 1966; Ahorner, 1972; Van Gils and Zaczek,

45   1978). Despite the consequences of this "past" seismic activity there is no published synthesis and specific analysis about its impact and the damage it caused. Providing an inventory of these effects and damage would be of great interest to identify the consequences of possible similar future activity, not only in the Hainaut area but also elsewhere in Western Europe in areas with a similar geological configuration. Such an investigation is required for the analysis of the possible impact of deep geothermal projects that are currently in test phase in the Hainaut coal area (https://geothermiemons.be).

50   The Hainaut seismic activity is of great concern for seismic hazard assessment in the border area between France and Belgium. This is particularly of interest for the Eurocode-8 norm application in Belgian and French building regulations because the contribution of Hainaut seismic activity in these hazard maps is significant (Fig. 1, Leynaud et al., 2001; Martin et al., 2002; Vanneste et al., 2014; Drouet et al., 2020). For the current hazard maps, two different aspects of this seismicity deserve specific research. First, the origin of this seismicity stays unresolved and controversial (Descamps, 2009; Troch, 2018a). In

55   hazard computations, natural seismicity would be a long-term stationary process, whereas seismicity induced by mining works would only be a past sporadic phenomenon. Hence, a reinterpretation on the origin would strongly modify its contribution to the seismic hazard. Second, in contrast to the observed strong intensity decay of these earthquakes, partly caused by the shallowness of the earthquake hypocentres, the influence area of the Hainaut seismicity seems too extended in the hazard maps. This inconsistency resulted from the use of inappropriate ground motion prediction equations (GMPEs) in hazard assessment.
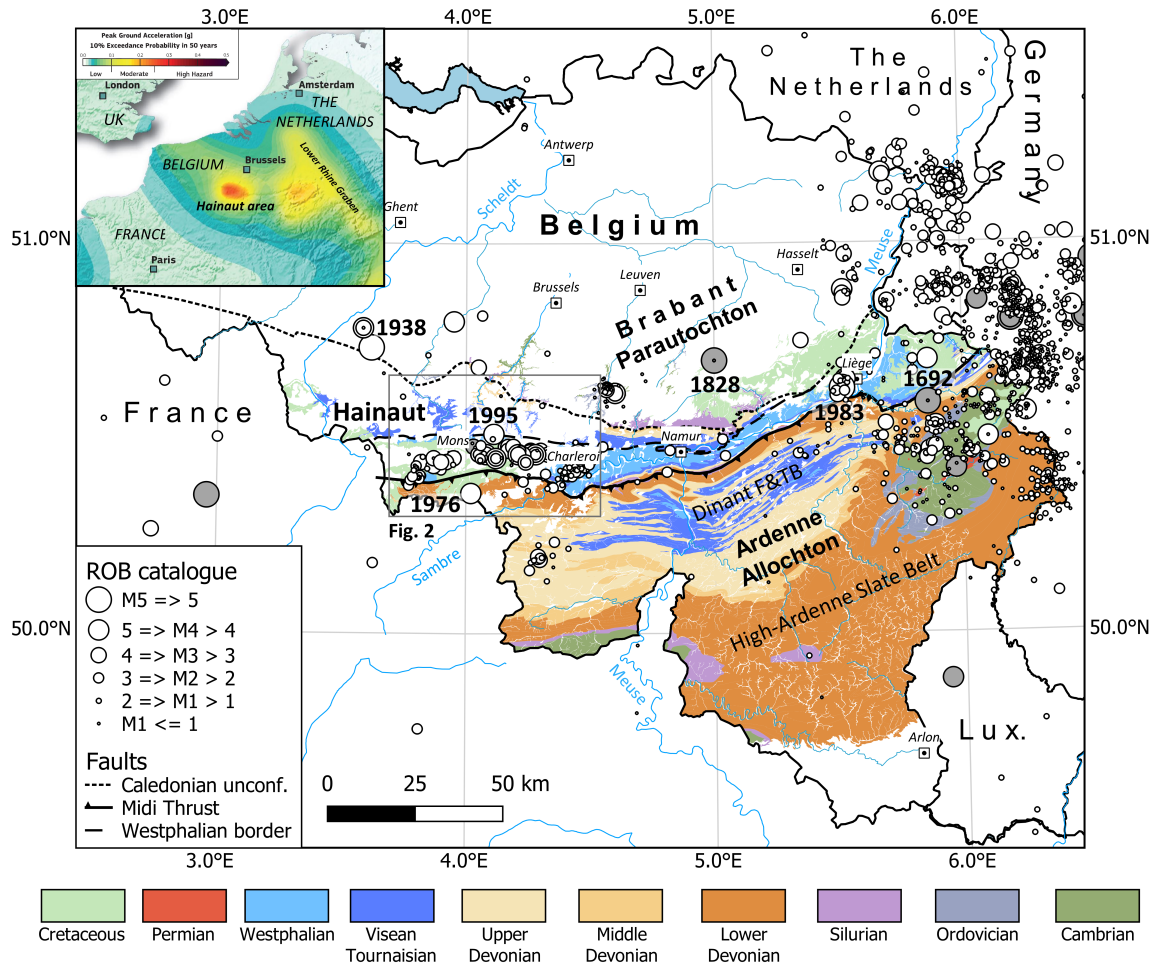
Figure 1. Regional seismicity and geological setting of the Hainaut coal area. Seismicity shown is the full seismic catalogue of the Royal Observatory of Belgium. Grey dots are historical earthquakes prior to the installation of the first seismometer in Belgium in 1911. The inset shows a zoom into the SHARE hazard map (Woessner et al., 2015) of the area around Belgium. Note the pronounced higher PGA exceedance in the Hainaut area based on the seismicity discussed in this paper. Geology in background based upon http://www.onegeology.org/. Reproduced with the permission of OneGeology. All rights Reserved.

Most of the earthquake activity in the Hainaut coal area occurred before the implantation of a modern digital seismic network in Belgium, which started in 1985 (Camelbeeck et al., 1990). Before the modern network, only the largest earthquakes have been recorded by seismic stations since 1909. Smaller events are only known because they were reported by people and (or) caused slight damage. Camelbeeck (1985a, b, 1993) and Camelbeeck et al. (1990) evaluated the magnitude of the largest events from seismic recordings. These studies underline the large uncertainties on earthquake locations from seismic phase measurements and conclude that for most events, the centre of the area with the largest observed intensity would better correspond to the real epicentre than the location obtained from arrival time measurements. Because of the uncertainty on focal depths, instrumental evaluations were only able to suggest that Hainaut events would certainly not exceed 7-8 km (Camelbeeck, 1990) and, to date, more accurate depth estimations are lacking. Macroseismic data are, however, a good and the only alternative to determine earthquake source parameters and tackle the context of this seismicity and related seismic hazard issues.

In this paper, we collected all available macroseismic data of this unique seismicity and searched for additional information providing a complete macroseismic intensity dataset of sufficient quality to estimate the impact and to answer the questions that the Hainaut seismicity raised. First, we explain how we established the full earthquake catalogue and the corresponding intensity dataset from the available (historical) sources of information and we provide a new earthquake catalogue of the Hainaut seismicity from 1887 to 1985. Second, we used the intensity dataset to develop a regional intensity attenuation relationship valid for the Hainaut coal area, which allows better estimating the earthquake focal depth, magnitude and epicentre location. We also compare the new Hainaut attenuation model with intensity datasets of other shallow, induced or triggered earthquakes worldwide. Finally, we discuss how our results should be incorporated in current seismic hazard studies. Appendix A presents the way we evaluated intensity from the available information sources. In Appendix B, a chronological description of the Hainaut seismicity is given. The macroseismic maps and a description of the sources of information concerning these earthquakes are presented in detail in an Atlas in the Supplement (further referred to as the Atlas). Communal intensity data points (IDPs) are provided for each earthquake in the Supplement.

2 Earthquake catalogue

The Hainaut earthquakes are included in the earthquake catalogue maintained by the Royal Observatory of Belgium (ROB; see Data Availability). The first earthquakes reported in the Hainaut coal area occurred in 1887 in the locality of Havré, a few km E of the city of Mons (Fig. 2), and were studied by de Munck (1887). The absence of scientific documentation before these events does not mean that small earthquakes could not have occurred prior to these events in the Hainaut coal area. However, at least since the beginning of the 19th century, it is doubtful that felt or damaging earthquakes would have escaped the attention of local authorities and the press because historical sources do report other 19th century earthquakes in neighbouring regions and describe their impact on Hainaut. An example is the 23 February 1828 M$_W$ = 5.1 earthquake in Central Belgium (Fig. 1) that was felt in underground mines in the Borinage and caused damage to chimneys in Gosselies (Camelbeeck et al., 2021).

To create the earthquake catalogue, Camelbeeck (1993) initially reviewed all the recordings of seismic stations in Belgium and neighbouring countries that could have reported phase arrival times and amplitude measurements for earthquakes
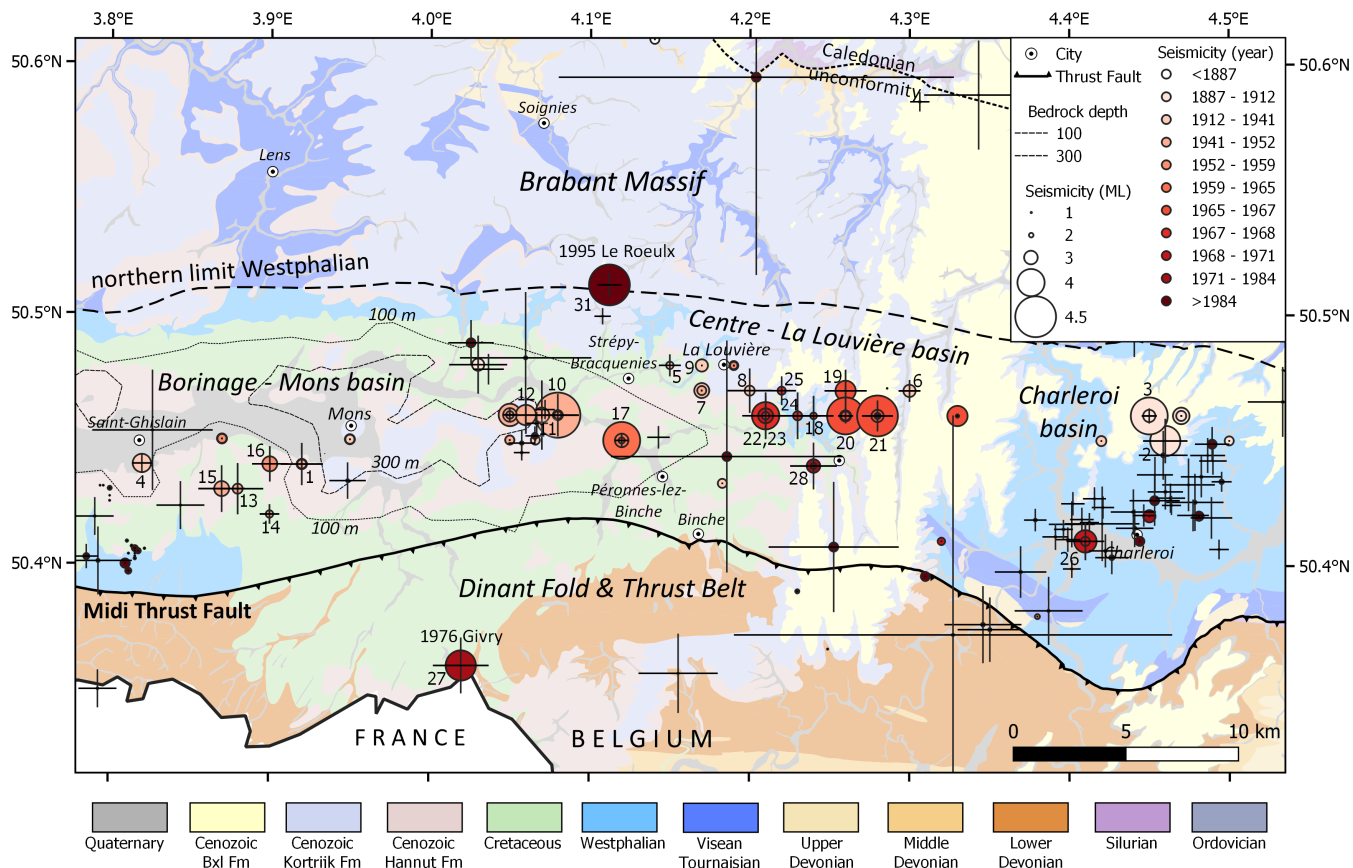
Figure 2. Geological setting of the 1887-2020 seismicity in the Hainaut province with local geological map as background. Borinage-Mons basin, La Louvière Basin and the Centrum Basin (Charleroi area) are the main coal regions in the Hainaut province. Seismicity (up to 2020) coloured in function of time and sized to magnitude. Black error bars show location uncertainty. Numbers next to the largest earthquakes refer to events in Table 1 and to macroseismic maps in the Atlas in the Supplement. Geology in background based upon http://www.onegeology.org/. Reproduced with the permission of OneGeology. All rights Reserved.

in Belgium. Between 1898 and 1958, the only seismic station in Belgium was Uccle (Brussels). Its capability to record local earthquakes was operational from 1909 onwards. However, the station was only sensitive enough to detect the largest earthquakes, and numerous felt earthquakes were too small to leave a trace on the black smoked or photo paper recordings. Hence, the ROB catalogue was extended by including felt Hainaut earthquakes that were not recorded by seismic instruments before 1958. However, their reporting is not homogeneous during this period. For the period between 1896 and 1936, Somville (1936) established a list including some events that were not recorded in Uccle but that were reported in press reports, in communications from local collieries or by local correspondents. The catalogue also contains non-instrumentally recorded aftershocks of the April 1949 Havré earthquakes reported in the press, and 12 earthquakes that occurred in the fifties and that were listed in the Belgian activity reports of the International Union of Geodesy and Geophysics (IUGG).

After 1958 and up to 1985, adding a few additional stations slightly improved the seismic monitoring in Belgium (Camelbeeck, 1985a). The higher sensitivity of the seismometers at the permanent stations in Dourbes and Membach, operating respectively since 1958 and 1977, allowed detecting smaller, even not felt, seismic events. Hence, from 1958, the bulletin of Belgian seismic stations includes all the potentially felt events. After 1985, the installation of a modern digital seismic network allowed the detection and precise location of $M_L > 1.0$ earthquakes in the Hainaut area (Lecocq et al., 2013) and in the southern part of the Brabant Massif (Van Noten et al., 2015). By the exception of weakly felt earthquakes in 1987 in the Dour area (Camelbeeck, 1988), no more events were sufficiently strong to be felt and the seismicity stayed at a very low level in Hainaut. Let's note that the $M_W = 4.1$ earthquake that occurred on 20 June 1995 had its epicentre near Le Roeulx, just north of the coal area (Figs. 1 and 2). With a focal depth of 25 km, the hypocentre was located in the lower crust of the Brabant Massif. It was felt on a large part of the Belgian territory and in northern France with an epicentral intensity of V (Fig. S31 in the Supplement).

Initially, we started our study using the list of Hainaut earthquakes reported in the ROB catalogue, but the new knowledge acquired in this study allowed us to complete this list and improve the location reliability and to evaluate the magnitude for all events. This resulted in an updated catalogue of 124 Hainaut earthquakes between 1887 and 1985 (see full catalogue in the Supplement) that is now fully integrated in the ROB catalogue. After 1985, the largest events that occurred in Hainaut are three M_L 2.5 earthquakes, which were only weakly felt. Earthquakes of magnitude below 2.0 occurred from time to time (31 earthquakes during the last 20 years), meaning that very little seismic energy was released in the coal area after the mining.

3 Macroseismic information and intensity evaluation

3.1 Sources of information

Our study is based on macroseismic information that is derived from various sources, including published scientific works contemporaneous with the earthquakes, the official macroseismic survey of the Royal Observatory of Belgium, press reports, letters to the ROB, and ROB, collieries company and administration reports. A detailed overview of these sources is provided in the Atlas in the Supplement.

Scientific studies have described the effects and (or) damage caused by some Hainaut earthquakes in large detail (de Munck, 1887; Cornet, 1911; Cambier, 1911; Capiau, 1920; Charlier, 1949; Marlière, 1951; Van Gils, 1966). Some works contain the

Table 1. *Parameter info of 28 Hainaut coal area earthquakes that have sufficient macroseismic data to be mapped (see Atlas). See Supplement for complete explanation of all catalogue parameters.* **Map:** *Atlas map number;* **ID_E:** *ROB catalogue number.* [inq]*: event with official ROB macroseismic inquiry;* **METHOD:** *method to compute macroseismic epicentre (G. Imax(-1): geocentre of the IDPs with Imax and Imax-1 intensities; G. Perc.: geocentre of all the IDPs);* **ERRH:** *Uncertainty on the reported epicentre in km;* **DEPTH:** *focal depth (km) estimated from the intensity attenuation modelling. Depths in brackets estimated from Imax;* **ERRZ:** *Focal depths (in km) using the Hainaut intensity attenuation relationship. Errors inside brackets estimated from Imax;* M_L: *Local magnitude determined Belgian station recordings;* M_S: *Surface-wave magnitude determined from European station recordings using the Prague formula (Kárník, 1971);* M_W_m: *Equivalent M_W determined from macroseismic data using the empirical relationships developed in this study;* M_W: *Moment magnitudes determined from Camelbeeck (1985). Magnitudes in brackets are converted from M_L;* **IMAX:** *maximum observed intensity;* **PERC.:** *Radius of perceptibility of the seismic event in km. R3: Radius of intensity III, R4: Radius of intensity IV;* **ERRM:** *Uncertainty on estimated magnitude;* **IDPs:** *Number of IDPs.*

MAP	ID_E	DATE	TIME	REGION	LAT	LON	METHOD	ERRH	DEPTH	ERRZ	M_L	M_S	M_W_m	M_W	IMAX	PERC.	ERRM	IDPs
S1	449	1911-04-12	16:15:–.–	CUESMES	50.44	3.92	G. Imax(-1)	1.8	[2.4]	[1.1]			3.1		4	5.4 R3	0.5 mac	22
S2	465	1911-06-01	22:51:58.–	RANSART	50.45	4.46	G. Imax(-1)	1.9	4.3	1.8	4.2	3.8		[3.9]	6	13.5 R4	0.3 M	53
S3	466	1911-06-03	14:35:54.–	GOSSELIES	50.46	4.45	G. Imax(-1)	0.6	[1.4]	[0.7]	4.4			[4.0]	7	7.7 R4	0.3 M	16
S4	476	1920-01-17	03:11:04.–	HORNU	50.44	3.82	G. Imax(-1)	0.8	[1.6]	[0.5]	3.7			[3.5]	6	5.3 R3	0.3 M	12
S5	488	1931-05-09	12:25:56.–	HOUDENG-AIMERIES	50.48	4.15	G. Perc.	0.9	[0.6]	[0.2]	2.8			[3.0]	4_5	2.5 R3	0.3 M	5
S6	505	1936-11-05	00:41:44.–	GOUY-LEZ-PIETON	50.47	4.3	G. Perc.	0.9	[2.2]	[0.9]			3.3		4_5	3.4 R4	0.6 mac	5
S7	517	1940-01-07	16:28:52.–	LA LOUVIERE	50.47	4.17	G. Imax(-1)	0.3	[1.5]	[0.6]			3.5		5	5.6 R3	0.5 mac	17
S8	518	1940-01-07	20:32:44.–	LA LOUVIERE	50.47	4.2	G. Imax(-1)	1.9					3.1		4	4.4 R3	0.5 mac	7
S9	519	1940-01-09	03:42:07.–	LA LOUVIERE	50.48	4.17	G. Imax(-1)	0.2	[2.8]	[1.4]			3.3		4_5	7.6 R3	0.5 mac	10
S10	534[inq]	1949-04-03	12:33:40.–	HAVRE-BOUSSOIT	50.46	4.08	G. Imax(-1)	1.8	2.2	0.8	4.6	4.3		[4.1]	7	18.0 R3	0.3 M	134
S11	538	1949-04-14	01:09:14.–	HAVRE-BOUSSOIT	50.46	4.07	G. Imax(-1)	3	[3.7]	[1.6]			3.5		5	8.5 R3	0.5 mac	15
S12	539	1949-04-14	05:12:21.–	HAVRE	50.46	4.06	G. Imax(-1)	1.6	[2.4]	[1.5]	3.8			[3.6]	6	9.5 R3	0.3 M	21
S13	547[inq]	1952-10-21	21:15:–.–	QUAREGNON	50.43	3.88	G. Imax(-1)	2.2	[2.9]	[1.9]			3.1		4	5.5 R3	0.5 mac	21
S14	548[inq]	1952-10-22	07:–:–.–	FRAMERIES	50.42	3.9	G. Imax(-1)	0.8	[3.0]	[1.0]			2.8		3	3.5 R3	0.4 mac	11
S15	549[inq]	1952-10-27	06:11:–.–	QUAREGNON	50.43	3.87	G. Imax(-1)	2	3.5	1.2			3.5		5	11.1 R3	0.5 mac	45
S16	562[inq]	1954-07-10	17:18:21.–	FLENU	50.44	3.9	G. Imax(-1)	1.5	3.3	1.2			3.5		5	8.8 R3	0.5 mac	44
S17	582[inq]	1965-12-15	12:07:15	STREPY-BRACQUEGNIES	50.45	4.12	G. Imax(-1)	0.5	2.7	0.8	4.4			4	7	20.7 R3	0.3 M	99
S18	587[inq]	1966-01-16	00:13:19	MORLANWELZ-MARIEMONT	50.46	4.24	G. Imax(-1)	1.7	[2.6]	[1.4]	2.7		[2.9]		4	7.2 R3	0.3 M	25
S19	588[inq]	1966-01-16	06:51:34	MORLANWELZ-MARIEMONT	50.47	4.26	G. Imax(-1)	1.8	3.3	1.6	3.8			3.5	5	8.5 R3	0.3 M	41
S20	589[inq]	1966-01-16	12:32:50	MORLANWELZ-MARIEMONT	50.46	4.26	G. Imax(-1)	0.6	2.1	0.9	4.4			4	7	24.9 R3	0.3 M	120
S21	597[inq]	1967-03-28	15:49:25	CARNIERES	50.46	4.28	G. Imax(-1)	1.3	3	1	4.5			4.1	7	29.3 R3	0.3 M	143
S22	603[inq]	1968-08-12	07:26:41	LA LOUVIERE	50.46	4.21	G. Imax(-1)	1.7	2.3	1	3.7			3.6	5	6.7 R3	0.3 M	29
S23	606[inq]	1968-08-13	16:57:14	LA LOUVIERE	50.46	4.21	G. Imax(-1)	2	2.3	0.8	4.1			3.9	6	11.5 R3	0.3 M	59
S24	607[inq]	1968-09-23	04:08:13	MORLANWELZ-MARIEMONT	50.46	4.23	G. Imax(-1)	2	2.8	1.7	3			3.2	5	6.2 R3	0.3 M	25
S25	608[inq]	1968-09-23	05:47:16	HAINE-SAINT-PIERRE	50.47	4.22	G. Imax(-1)	1.2	[2.4]	[1.1]	2.9			3	4	4.7 R3	0.3 M	25
S26	612[inq]	1970-11-03	08:46:00	MARCHIENNE-AU-PONT	50.41	4.41	G. Imax(-1)	1.6	2.3	1	3.9			3.6	5	9.8 R3	0.3 M	31
S27	627[inq]	1976-10-24	20:33:28	GIVRY	50.36	4.02	G. Imax(-1)	2.4	5.5	1.7	4.2			[3.9]	6	16.0 R3	0.3 M	95
S28	641[inq]	1982-09-14	19:24:35	CARNIERES	50.44	4.24	G. Imax(-1)	2	[3.5]	[1.6]	3.4			[3.4]	4	6.9 R3	0.3 M	18

own observations of the author(s), complemented by testimonies collected by interviewing local people, similar as today's Macroseismic Intervention Group (Sira, 2015) would do.

Macroseismic surveys are indispensable to map an earthquake's impact. They serve to evaluate the earthquake's magnitude and focal depth, the intensity-distance decay, and the impact of the local geology on the macroseismic field (Cecić and Musson, 2004). Since 1932, the ROB organises a macroseismic survey whenever an earthquake is felt in Belgium. For the Hainaut earthquakes, the surveys consisted of sending a dedicated questionnaire to the burgomasters of Belgian communes up to 50 km from the epicentres asking them to carefully report the earthquake observations. Between 3 April 1949 and 9 August 1983, 19

official ROB surveys were organised in Hainaut. 17 of them were usable to evaluate the intensity for each locality (indicated with ^{inq} in Table 1) in the EMS-98 macroseismic scale (Grünthal et al., 1998) and to compose a macroseismic map (see Atlas).

135 Intensities gathered from official surveys provided convincing results because municipalities in Belgium were small (mean area size of only 19 km^2) and numerous (2359 communes). After the big community fusion in 1977, in which Belgium changed from 2359 to 596 communities (with mean area size of 82 km^2), macroseismic surveys of more recent earthquakes lost the quality and resolution they once had because the new communities cover a too large area to be represented by only one intensity value.

140 At the end of the 19th century and beginning of the 20th century, local and regional press reports were very beneficial documents for seismologists to summarise an earthquake's impact (Alexandre et al., 2007; Camelbeeck et al., 2021). In addition to the press information already present in the ROB database, we consulted La Louvière record-office collections and scanned press archives of the State Archives of Belgium (2021) to extend our knowledge on the Hainaut earthquakes. The list of consulted newspapers is presented in the Atlas.

145 Additional information comes from letters of individuals or small reports addressed by the collieries companies to the ROB at the time of the mining exploitation (Somville, 1936). The ROB also organised field missions after the 3 April 1949 [id 534] and 10 July 1954 [id 562] earthquakes to provide epicentral damage reports.

3.2 Intensity evaluation

Based on the sources mentioned above, we re-evaluated local intensities for each earthquake at each locality. Intensity is
150 determined in the EMS-98 scale, the current standard in Europe. Its great advantage is the use of building vulnerability classes allowing integrating the current state of the building stock in the intensity determination (Grünthal et al., 1998). The background how we evaluated building vulnerability and assessed intensity is explained in Appendix A. As it was not always possible to precisely evaluate intensity to a single integer value, we provide for each IDP two intensity values, i.e. minimum (Imin) and maximum (Imax) intensity, corresponding to the possible range of the intensity evaluation.

155 3.3 The Hainaut intensity dataset

Based on the intensity evaluation, we created individual files that contain the communal intensity data points (IDPs) for each earthquake. For each of the 17 earthquakes for which the ROB official survey is usable to evaluate local intensities, we composed an inquiry book presenting the English translation of the communal replies to the ROB questionnaire. Using these books, the reader can examine the effects of each earthquake at each location. The IDP files and the inquiry books are included in the
160 Supplement.

In Table 1, we give a chronological overview of 28 earthquakes that were widely felt or caused damage in the Hainaut coal area. For each of these 28 events, the impact and magnitude estimation is described in Appendix B. We also summarise the intensity information, the intensity barycenter and the epicentral population density of these events in a macroseismic map and provide these in Appendix B and in the Atlas. An example of these maps is shown in Figure 3. Because newspapers often

165 report precise addresses or places in cities where some specific damage occurred, we geocoded this information and report the type of damage on the macroseismic maps.

All this information composes a significant intensity dataset that is summarised in Table 2. This table presents the number of IDPs for each intensity unit computed by taking the mean of Imin and Imax values for the different localities.

Table 2. Summary of intensity (EMS-98) data for the largest earthquakes in the Hainaut coal area and which mapped in the Atlas. Map: map number in Supplement. Total IDPs: Amount of IDPS with mean intensity of Imin and Imax. Inq: earthquake with an official ROB intensity survey; *: earthquake used for Hainaut intensity attenuation modelling.

Map	id_earth	Date	F	II	II-III	III	III-IV	IV	IV-V	V	V-VI	VI	VI-VII	VII	Total
S1	449	1911-04-12		2	3	14	2	1							22
S2	465*	1911-06-01				2		31		14	2	4			53
S3	466	1911-06-03	11					2		1		1		1	16
S4	476	1920-01-17	9							1		2			12
S5	488	1931-05-09	4						1						5
S6	505	1936-11-05							5						5
S7	517	1940-01-07			2	6	5	3		1					17
S8	518	1940-01-07	7												7
S9	519	1940-01-09	5			2		2	1						10
S10	534^{inq,*}	1949-04-03		24	3	36	1	32	8	13	6	7	2	2	134
S11	538	1949-04-14	7					6		2					15
S12	539	1949-04-14	12						2	3	2	2			21
S13	547^{inq}	1952-10-21		2	1	12	2	4							21
S14	548^{inq}	1952-10-22		1	1	7	1	1							11
S15	549^{inq}	1952-10-27		6		13	4	12	2	8					45
S16	562^{inq,*}	'1954-07-10		11		7	1	9	2	12	2				44
S17	582^{inq,*}	1965-12-15		23		30	6	17		19		2		2	99
S18	587^{inq}	1966-01-16		3	1	13	4	2	2						25
S19	588^{inq,*}	1966-01-16		15	1	8	2	12	1	2					41
S20	589^{inq,*}	1966-01-16		37		42	2	22	1	12		3		1	120
S21	597^{inq,*}	1967-03-28		40		56	3	22	1	10		9		2	143
S22	603^{inq,*}	1968-08-12		6		2	1	12		8					29
S23	606^{inq,*}	1968-08-13		18		9		10		17	1	4			59
S24	607^{inq,*}	1968-09-23		10			4	9	1	1					25
S25	608^{inq}	1968-09-23		13		5	2	5							25
S26	612^{inq,*}	1970-11-03		6		9	3	5		8					31
S27	627^{inq}	1976-10-24		24		24	1	33	1	10		2			95
S28	641^{inq}	1982-09-14		1	1	8	1	7							18
Total Intensity			55	242	13	305	45	259	28	142	13	36	2	8	1148
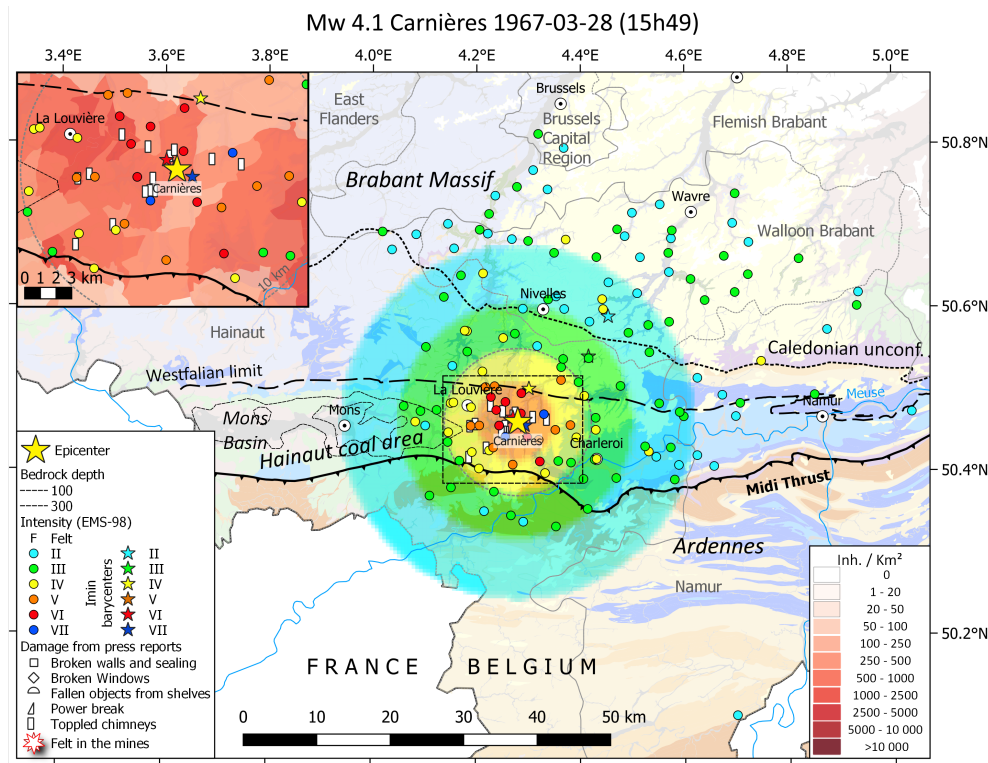
Figure 3. Intensity information of Hainaut events is represented in macroseismic maps such as for the 1967 M_W=4.1 (M_L=4.5) Carnières earthquake (nr 21 in Table 1). The inlet shows localities where specific damage has been reported in press reports. Note the asymmetric macroseismic field: this event has been felt more northwards within the borders of the Brabant Massif, than southwards in the Ardennes, which results in a northwards shift of the lower intensity (Imin IV, III and II) barycentres. In the background, the Hainaut intensity attenuation model developed in this study (see section 4.2) is applied to the parameters of this event. Note that this attenuation model only can be applied within the coal area (between the Midi Thrust and Westfalian limit). Modelled Imax = VI, but locally intensity VII is observed. See the Atlas in the Supplement for other events.

4 Intensity attenuation and focal depth estimation

170 Seismic intensity is an empirical measure of the severity of ground motions generated by earthquakes. Determining intensity inside the radius of an earthquake's perceptibility allows mapping ground motion strength and its spatial variability. The macroseismic field directly relates to earthquake epicentre location, focal depth and magnitude, and near-field energy absorption coefficient (Ambraseys, 1985). Hence, determining the parameters controlling seismic energy absorption offers the possibility to evaluate the location and magnitude of past earthquakes from their intensity spatial distribution (Sbarra et al.,

175 2019; Provost and Scotti, 2020). Creating an attenuation model also gives the possibility to predict intensities for a specific earthquake with given focal depth and magnitude.

4.1 Methodology

Ambraseys (1985), Hinzen and Oemisch (2001), Bakun and Scotti (2006), and Stromeyer and Grünthal (2009) developed regional intensity attenuation models using earthquake datasets from Western and Central Europe. Except for Ambraseys (1985), who used isoseismal radii, these authors all based their models on IDP distributions. Knuts et al. (2016) and Camelbeeck et al. (2021) successfully applied these models to determine epicentral locations and magnitudes of historical earthquakes in Belgium. Even though these datasets include information on very shallow earthquakes, the small number of shallow events with respect to deep ones, makes these models less suitable to simulate the macroseismic field of shallow earthquakes. However, seismic attenuation characteristics are more variable in the fractured upper layers of the crust because of large lateral variations of mechanical characteristics of rocks and sediments near the surface. Hence, for shallow earthquakes, it would be more appropriate to develop a new local intensity attenuation model than using these Western and Central Europe models. Moreover, given the large available intensity dataset for the Hainaut coal area, it would be even more realistic (Table 2).

To develop a local Hainaut intensity attenuation model, we used the classical formulation developed by Kövesligethy (1907) and still widely used today (e.g. Ambraseys, 1985; Stromeyer and Grünthal, 2009):

$$I = I_0 - a * log(\sqrt{\frac{R^2 + Z^2}{Z^2}}) - b * (\sqrt{R^2 + Z^2} - Z) \tag{1}$$

where I is the intensity at epicentral distance R from an earthquake source at focal depth Z, I_0 is the epicentral intensity. a and b are parameters that respectively correspond to the multiplication of the geometric spreading and energy absorption factors by the proportionality factor between intensity and ground motion acceleration (Ambraseys, 1985; Stromeyer and Grünthal, 2009). a and b can be derived by fitting Eq. 1 to IDPs of calibration earthquakes with a well-determined location and focal depth. Solving the parameters of Eq. 1 using intensity datasets can performed by three different approaches: (1) using intensities and epicentral distances of all individual observations; (2) using the mean distance and its standard deviation by intensity binning; and (3) using the mean intensity and its standard deviation by distance binning (used in this work).

4.2 Intensity attenuation in the Hainaut coal area

Figure 4 presents an example for the 15 December 1965 earthquake (macroseismic map on Fig. B4) and shows how IDP epicentral distance binning is applied. For each distance bin of 2.5 km, the diagram reports the mean intensity minus I_0 (determined from the IDP distribution - see further in this section) and its standard deviation, representing the intensity variability inside the distance bins. The number of IDPs in each bin progressively increases up to a distance of 15 km from the epicentre and then abruptly decreases. Beyond this distance, there are only a few IDPs, which are of low intensities, which indicates that the earthquake was likely not felt in many localities contributing to these bins. This suggests that the mean values computed from these IDPs would overestimate the mean intensity of the bins because "not felt" localities are not included in the computation. This example also shows the rapid intensity decrease with increasing distance in the coal area (Fig. 4), which for the 15 December 1965 earthquake corresponds to a decrease of three intensity grades on a distance range of 15 km. North of the Hainaut coal area, inside the borders of the Brabant Massif (see e.g. Figs. 3, B2 and B4), the largest earthquakes are weakly
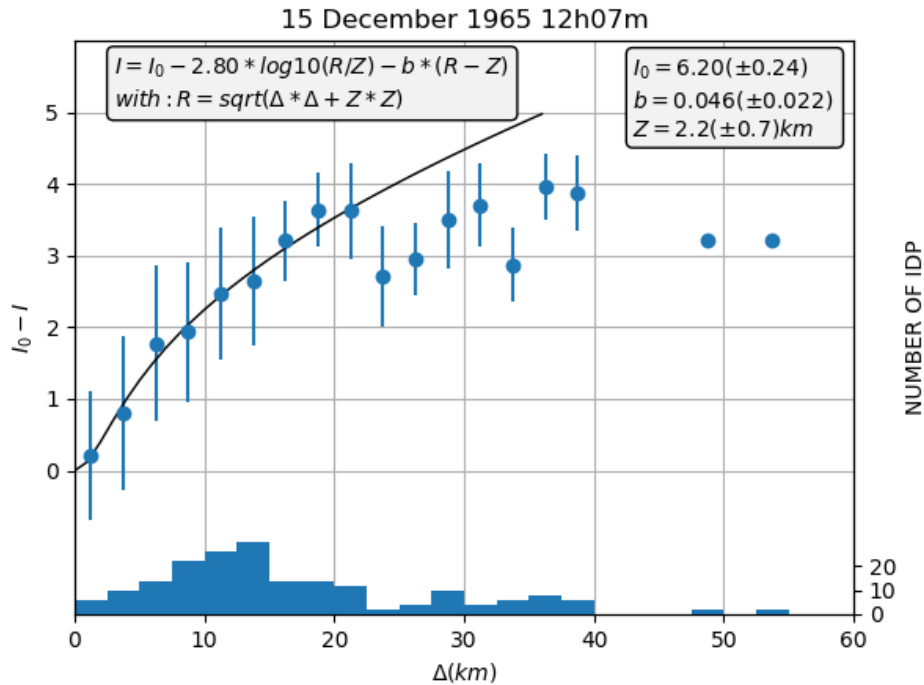
Figure 4. Intensity attenuation of the 15 December 1965 Strépy-Bracquegnies earthquake expressed as mean intensity change relative to I_0 (blue dots) calculated for bins of 2.5 km (histogram). Vertical blue bars show intensity standard deviation for each distance bin that expresses the intensity variability in the bin. The legend reports local parameters fitting the intensity attenuation of Eq. 1 with a fixed to 2.80.

felt with intensity II to III up to a distance exceeding 40-50 km, suggesting a slower intensity attenuation than in the coal area.
210 South of the Hainaut coal area, the Midi fault (Fig. 2) seems to play the role of a seismic barrier and intensity decays more rapidly in the Ardenne Massif than in the Brabant Massif, conform the observation of Charlier (1951).

IDPs at distances larger than 15 km should hence not be used to analyse intensity attenuation in the coal area because: (1) IDPs beyond these distances bias the mean intensity values in the bins, and (2) the intensity attenuation of the coal area differs from attenuation in the Brabant Massif and in the Ardenne. Hence, applying a distance range larger than 15 km would not
215 properly model the attenuation in the coal area, but would provide an intermediate attenuation including crustal characteristics from these three areas. We prefer distance binning of intensity with small bins of 2.5 to 3 km over intensity binning as it provides more data points, which is more appropriate to invert parameters a and b of Eq. 1. For example, for the 15 December 1965 earthquake (Fig. 4), the mean intensities of 6 distance bins within 15 km provide a more robust fit with Eq. 1 than the mean distances of 4 intensity bins, covering 3 intensity units, would do.
220 The dataset used for the attenuation modelling is relatively small, with 76 mean intensity values obtained by distance binning of 12 key earthquakes. In our computation we also included two additional events (identified by an ° symbol in Table 3) because,
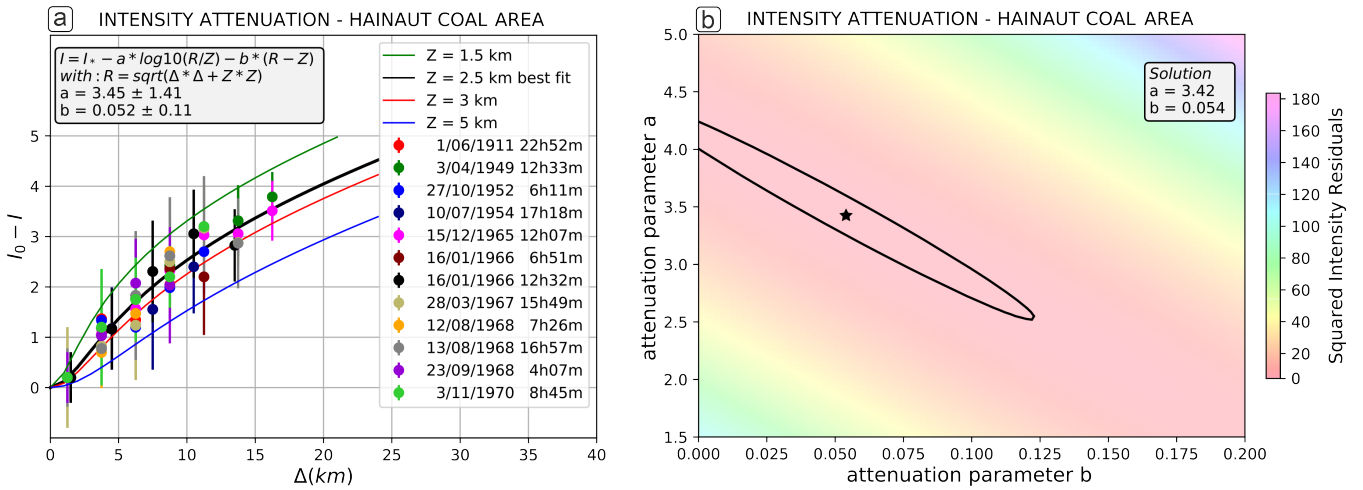
Figure 5. a) Fitting the intensity dataset of 12 calibration earthquakes to Eq. 1 to determine a and b attenuation parameters and the focal depth considering a uniform depth for all events. b) Least-squares fitting by sampling the a and b intensity parameters space: the solution is represented by the star and the black ellipse limits the 0.95 confidence region.

although they occurred outside the Hainaut coal area, the geological context of the felt observations is similar to the earthquakes that occurred inside the Hainaut coal area. These two events are the 24 October 1976 earthquake (Fig. S27), which occurred a few km south of the Hainaut coal area, and the 8 November 1983 Liège earthquake (Fig. S29 Camelbeeck, 1993; Camelbeeck et al., 2021) that occurred in the Liège coal area, in a similar geological context as Hainaut.

The main hypothesis in our fitting analysis is that intensity attenuation is homogeneous in the Hainaut coal area, which means that the parameters a and b have the same values for all seismic events in the area. Hence, the observed variations in the intensity decay with increasing distance between the different calibration earthquakes are only associated with a difference in focal depth, in the uncertainty of the attenuation model and in the data. We determine parameters a and b in two steps:

1. As focal depth is unknown for the calibration earthquakes, a first step in the analysis was to evaluate their depth by fitting each earthquake dataset to Eq. 1 (see macroseismic maps in the Atlas). As Eq. 1 has four unknowns and the number of distance bins for each earthquake does not exceed seven, we fixed the value of the parameter a, and inverted the equation to evaluate the attenuation parameter b, the earthquake focal depth Z and epicentral intensity strength I_0. We considered that b is more dependent on the highly variable material properties near the Earth's surface than a, which should be relatively similar in Hainaut than elsewhere in Europe. We adopted the value $a = 2.80$ of the WLQ model of Stromeyer and Grünthal (2009). Table 3 reports the results of this analysis. Our main conclusion is that all the studied Hainaut earthquakes have similar focal depths ranging between 1.6 and 4.0 km, with uncertainties around 1.5 km.

2. In the second step, we considered that the 12 calibration Hainaut earthquakes have the same focal depth, which is supported by the results of the first step of the analysis. Based on the results of the first step, we fixed the value of I_0 by considering that the mean intensity of the first distance bin of each earthquake equals $I_0 - 0.3$. We represent this

estimation of I_0 by I^*. Then, we inverted the complete dataset to evaluate a, b and the focal depth, i.e. identical for all the earthquakes, which minimised the residuals by a Least-squares modelling. Figure 5a presents the results of this inversion in which a=3.45±1.41 and b=0.052±0.11, while the focal depth that best fits the data is 2.5 km.

Table 3. *Depth evaluation of calibration earthquakes used for attenuation modelling. I_0: epicentral intensity; Z: depth; b: attenuation parameter b; step: length of distance bin in km; n: number of distance bins.* [1]*first step of the analysis in which parameter a is held constant at a value of 2.80;* [2]*second step of the analysis.* °*earthquake not included in the attenuation modelling but used for verifying the model.*

id_earth	Date	Time	Lat (°N)	Lon (°E)	$I_0^{(1)}$	Z (km)$^{(1)}$	$b^{(1)}$	$I_0^{(2)}$	Z (km)$^{(2)}$	step	n
465	1911-06-01	22h52m	50.46	4.46	6.15±0.14	2.4±0.6	0.010±0.026	5.91±0.48	4.3±1.8	2.5	5
534	1949-04-03	12h33m	50.45	4.07	7.24±0.37	1.7±0.8	0.064±0.034	6.95±0.52	2.2±0.8	2.5	7
549	1952-10-27	06h11m	50.44	3.9	5.29±0.37	2.3±1.2	0.022±0.045	5.03±0.41	3.5±1.2	2.5	6
562	1954-07-10	17h18m	50.46	3.88	5.43±0.37	2.3±1.1	0.060±0.032	5.39±0.44	3.3±1.2	3	5
582	1965-12-15	12h07m	50.45	4.09	6.20±0.24	2.2±0.7	0.046±0.022	6.19±0.47	2.7±0.8	2.5	7
588	1966-01-16	06h51m	50.46	4.23	4.86±0.19	2.1±0.6	0.023±0.030	4.77±0.56	3.3±1.6	2.5	5
589	1966-01-16	12h32m	50.47	4.26	6.00±0.19	3.1±0.9	0.150±0.039	6.23±0.66	2.1±0.8	3.5	5
597	1967-03-28	15h49m	50.45	4.27	6.68±0.79	1.8±1.7	0.112±0.073	6.21±0.47	3.0±1.0	3	7
603	1968-08-12	07h26m	50.45	4.21	5.33±0.29	2.0±0.7	0.088±0.030	5.44±0.70	2.3±1.0	3	4
606	1968-08-13	16h57m	50.46	4.23	5.81±0.27	4.0±1.9	0.162±0.067	6.01±0.54	2.3±0.8	2.5	6
607	1968-09-23	04h07m	50.46	4.23	4.68±0.39	2.1±1.4	0.048±0.098	4.76±0.76	2.8±1.7	2.5	4
612	1970-11-03	08h45m	50.4	4.41	5.16±0.35	3.2±2.1	0.089±0.093	5.29±0.63	2.3±1.0	2.5	5
627°	1976-10-24*	20h33m	50.36	3.98	5.08±0.23	4.0±1.5	0.036±0.026	5.13±0.38	5.5±1.7	3	5
641°	1983-11-08*	00h49m	50.63	5.51	7.13±0.18	3.3±0.9	0.044±0.017	6.91±0.28	5.7±1.5	3	7

The relative small number of data and the lack of information at distances larger than 20 km cause the large uncertainties on a and b. However, it relies on their relative dependence which is well illustrated by their joint confidence region in Figure 5b. Figure 6 presents the intensity attenuation curves corresponding to the best solution and the two extreme solutions at the 0.95 confidence region for focal depths ranging from 1 to 6 km. The difference between these models for a given focal depth is very small for distances less than 15 km, i.e. 0.3 intensity units for a distance of 20 km, but becomes more important at larger distances. The uncertainty on the two parameters reflects the fact that a controls the short distance behaviour and is better determined while b characterises the curves at large distance.

4.3 Earthquake focal depth

Figure 6 reports the influence of focal depth from 1.0 to 6.0 km on the intensity attenuation curves. Changing focal depth has a stronger effect on the attenuation function than the uncertainties on the attenuation parameters. This observation indicates that focal depth can be evaluated with a good accuracy using IDPs and that the differences in attenuation observed between the different earthquakes in the modelling (Fig. 5a) reflect the small differences in their respective focal depths. Subsequently, we used the new Hainaut attenuation model to estimate the focal depth and the epicentral intensity of the 12 reference earthquakes
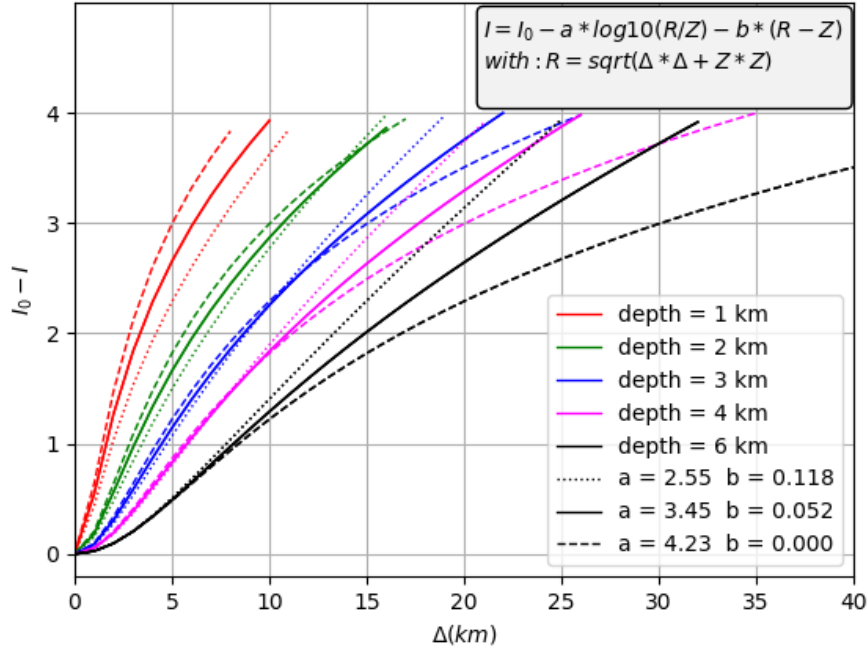
Figure 6. Variation of I_0 - I in function of epicentral distance corresponding to intensity attenuation models of Figure 5. The curves correspond to the best fitting solution (full lines) and the two extreme solutions (dotted and dashed lines) at the 0.95 confidence region for focal depths ranging from 1 to 6 km.

in the Hainaut coal area and the 1976 and 1983 Liège earthquakes. Figure 7 presents the results of this modelling for the 15 December 1965 earthquake. In the Atlas, the same diagram is provided for the 13 other earthquakes. For earthquakes other than the 12 calibration events in Table 1, macroseismic datasets are less complete and the full modelling cannot be applied.

260 Nevertheless, the available information is sufficient to correctly evaluate focal depth for most of them. For each event, the input data for focal depth determination are Imax, the maximal observed intensity, and the intensity I and epicentral distance Δ for each observed IDP. For each of these events, we created 250 different datasets by adding a random noise with possible values of -0.5, 0 or +0.5 to the intensity I of the IDPs, which would represent the uncertainty on each intensity evaluation. For each of the modelled IDPs, we searched the focal depth Z minimizing $I - I_{Max} = -3.45 * log(\Delta/Z) - 0.052 * (\Delta - Z)$ by testing

265 focal depths in a range of 0.1 km from 0 to 10 km. The computed mean focal depths and the sigma value of the distribution from the 250 different models for each earthquake are indicated in Table 1 inside brackets. For some other earthquakes, like the 1887 Havré and 1904 Fleurus events, or events that occurred between 1950 and 1960, only slight damage was reported and too few IDPs are available to compute their depth. However, from the estimations of Imax and the published perceptibility radius, we can still evaluate their focal depth by directly plotting the perceptibility radius in function of the observed intensity
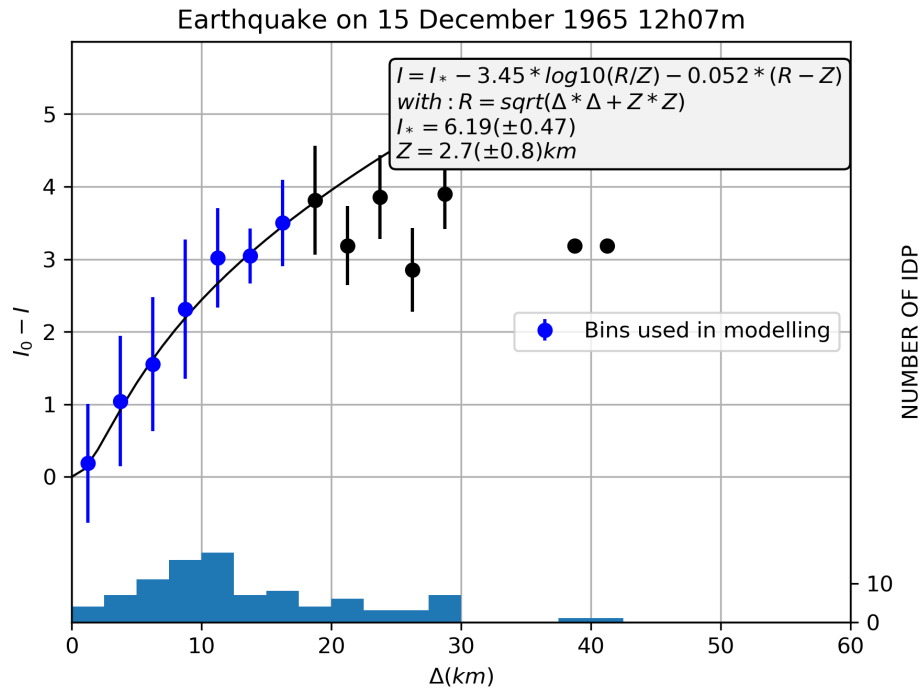
Figure 7. Evaluation of focal depth and epicentral intensity for the 15 December 1965 Strépy-Bracquegnies earthquake. The first seven distance bins (blue) are used in the modelling. Similar diagrams are provided in the Atlas for the 13 other earthquakes for which this method was used.

270   decrease, as represented in Fig. 6. Results show that most of these events are very shallow. For these events, we indicate the estimated focal depth inside brackets in the full catalogue in the Supplement, but without any uncertainty.

5   Instrumental magnitudes and magnitude determined from macroseismic data

Camelbeeck (1985a, 1993) determined the local magnitude M_L of the Hainaut earthquakes between 1911 and 1985 when the seismic measurements from at least one seismic station were available. For some events, it was also possible to determine

275   surface wave magnitude M_S using the Prague formula of Kárník (1971). Camelbeeck (1985b) estimated seismic moments and M_W for 17 earthquakes that occurred between 1965 and 1970 in the Hainaut coal area based on the coda waves enveloppe measured on the paper recordings from the Belgian seismic station of Dourbes. Even if the absolute value of these seismic moments were dependent on approximate parameterisation of the scattering properties of the crust between the coal area and the town of Dourbes, the used method furnishes a reliable ratio of the seismic moment values between the different earthquakes.

280   Denieul (2014) used the recordings of the CEA-LDG (Commissariat à l'Energie Atomique, Laboratoire de Détection et de Géophysique, France) seismic network to determine moment magnitudes of significant earthquakes in France and surrounding

regions that occurred from 1963 to 2013. This study determined M_W for the three earthquakes in Hainaut that occurred on 15 December 1965 at 12h07m, 16 January 1966 at 12h32m and 28 March 1967 at 15h49m as respectively 4.0, 4.0 and 4.1, with a one sigma uncertainty of 0.2. These results suggest that the moment magnitude determined from Camelbeeck (1985b) should be diminished by a constant factor of 0.3 magnitude units. This result also allows re-evaluating the relationship between M_L and M_W for the Hainaut earthquakes furnished by Camelbeeck (1985b) as:

$$M_W = 1.294(\pm0.08) + 0.610(\pm0.059) * M_L \tag{2}$$

which is valid between M_L=2.6 and M_L=4.6.

We reported in Table 1 the instrumental magnitude values that were determined for earthquakes in the Hainaut coal area. In addition, we used Eq. 2 to estimate M_W for the earthquakes for which only M_L was determined. For those events, the M_W value and its uncertainty are indicated inside brackets, while M_W determined from Camelbeeck (1985b) modified by Denieul (2014) are reported with their uncertainty without brackets. Thanks to the fact that instrumental magnitudes were determined for a part of the earthquakes for which macroseismic data are available, we were able to establish relationships between earthquake magnitude and macroseismic parameters. This allows determining a formula for a robust evaluation of earthquake magnitude M_W directly from macroseismic information for events that were not recorded by seismic stations.

We used the classical model (Sponheuer, 1962; Van Gils and Zaczek, 1978; Ambraseys, 1985; Stromeyer et al., 2004):

$$M = a * I_0 + b * log(h) + c \tag{3}$$

which determines the magnitude knowing epicentral intensity I_0 and focal depth h. As the range of focal depth in our calibration dataset of 12 earthquakes is limited around 2.5 km (Figure 6), it was not possible to find a reliable relationship with focal depth. However, I_0 is a parameter resulting from the fitting of IDPs with Eq. 1 and hence cannot be determined for earthquakes with only few IDPs (e.g. for 19th or first half of 20th century earthquakes or aftershocks of strong earthquakes). In this case, the only available parameter is the maximal observed intensity Imax (see Table 1). For this reason, we established a relationship between M_W and Imax (Fig. 8) rather than I_0 so that a specific model can be used for earthquakes with few macroseismic observations:

$$M_W = 1.744(\pm0.130) + 0.346(\pm0.098) * I_{max} \tag{4}$$

This relationship is certainly valid for earthquakes with focal depths in the range 1.5 to 4.0 km as the ones in our calibration dataset and their associated seismic sequences, but it would overestimate the magnitude for earthquakes closer to the surface. Considering that geometrical spreading would play a more significant role in seismic waves energy attenuation from the earthquake depth to the epicentre at the surface and that body waves are a major part of the radiated energy to the surface, b is fixed to 2.0 in Eq. 3.

Hence, for earthquakes shallower than 1.5 km, we determined M_W using the relationship:

$$M_W = 0.948(\pm0.130) + 2.0 * log(h) + 0.346(\pm0.098) * I_{max} \tag{5}$$
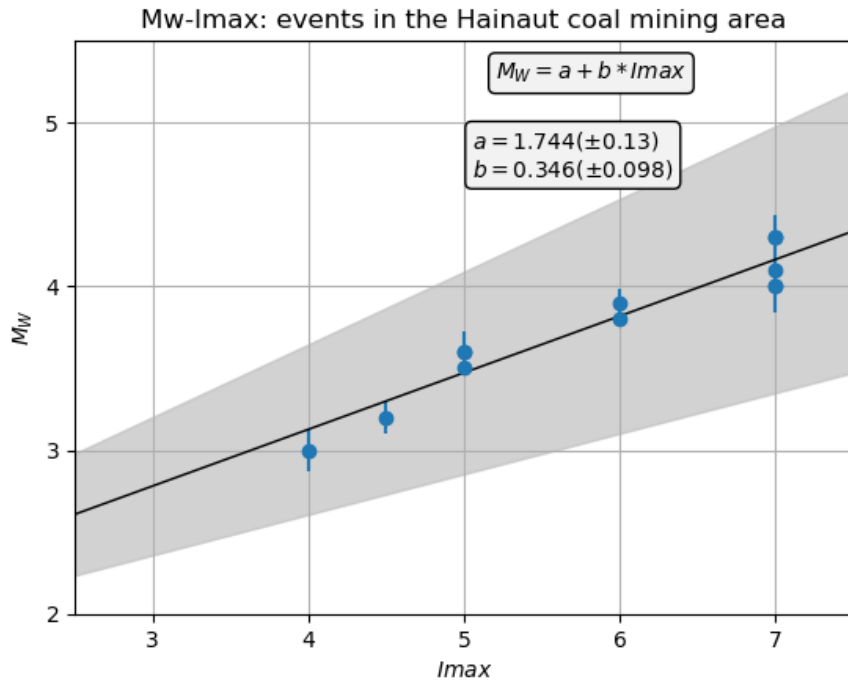
Figure 8. Relationship between M_W and Imax (approximation for I_0) determined for 12 calibration earthquakes in the Hainaut coal area (three data points are not visible because they are superposed above each other).

In Table 1, all the earthquakes for which M_W was determined using macroseismic information and Eq. 4 or Eq. 5 are reported in column M_W_m.

6   Discussion

In this discussion, we emphasise four aspects of the seismicity that occurred in the Hainaut coal area between the end of the 19th century and 1985. First, we compare the impact and intensity attenuation of the Hainaut earthquakes with the ones of shallow earthquakes with similar magnitudes in other regions of the world. Second, we describe the cumulative impact of the Hainaut coal area seismicity and compare it to the effects of a few larger magnitude 20th century earthquakes on the Hainaut area, suggesting that the Hainaut seismicity could be overestimated in current seismic hazard maps. Third, we discuss the pertinence of our new Hainaut intensity attenuation relationship in the light of the spatial resolution of our intensity dataset and the local and regional geological configuration. Last, we underline the importance of our focal depth determinations to discuss the causality of seismicity in and around the Hainaut coal area.

6.1 How fast is the Hainaut attenuation?

325 Our study brings out that the Hainaut events were locally damaging when M_W was greater than 3.5, and that damage stayed spatially limited because intensity decreased fast, by two grades in a range of distances from a few to a maximum of 7-8 km from the epicentre (Fig. 6). In the perspective of seismic hazard issues, it is relevant to evaluate whether or not this attenuation and the spatial extension of damage are similar in other regions worldwide where shallow seismicity occurs. To tackle this question, we compare in Figure 9a and b the intensity datasets of M_W 3.5 and M_W 4.0 earthquakes in Hainaut with shallow

330 earthquakes of similar magnitude induced or triggered by gas extraction (Groningen gasfield, NL, Dost and Kraaijpoel, 2013) or waste water injection (Oklahoma, US, Atkinson, 2020). We also report the Hainaut intensity attenuation curve on these two diagrams, as well as on Figure 9c, which represents M_W 5.0 earthquakes induced or triggered by potash and salt mining (Völkerhausen, DE, Leydecker et al., 1998) or rock removal above a pre-stressed fault (Le Teil, FR, Sira et al., 2019).

In this analysis, we compute the mean intensity decay and its standard deviation for hypocentral distance bins of 3 km

335 through the individual datasets. The main result is that, regardless of the magnitude, the mean intensity and the mean plus one standard deviation of the bins for events elsewhere in the world are larger than the Hainaut attenuation relationship and most of the Hainaut bins. This is clearly visible at large distance (Fig. 9) and is very likely associated to the location of the Hainaut coal deposits in the frontal zone of the Variscan tectonic belt. In this region, strong attenuation can be associated with the combined effect of a high fracturing degree of the subsurface and a low Q-factor associated to the slow propagation velocity of

340 coal deposits.

At short distance, it is difficult to discriminate a real difference in the mean value and the mean value plus one sigma of the intensity bins for magnitudes M_W 3.5 and M_W 4.0. Nevertheless, despite their greater focal depth, the bins of the Huizinge earthquake (depth=3 km) and Oklahoma events (depth=5 km) show similar or slightly greater values than the ones for Hainaut events (mean depth of 2.5 km), suggesting a slightly more damaging impact than in Hainaut. Moreover, if an earthquake of

345 magnitude around M_W 5.0 would have occurred in Hainaut, our analysis shows that its impact would have been smaller than the impact of the very shallow Le Teil 2019 and Völkerhausen 1989 seismic events. For these two events, the radius in which the mean intensity is larger than V, is twice as large as the intensity V radius of the Hainaut earthquakes.

6.2 The impact of the Hainaut seismic activity

The macroseismic maps in the Supplement present the impact and the importance of damage caused by the different earth-

350 quakes that stroke the Hainaut area between 1887 and 1985. The analysis presented in Figure 9, in which the intensity distribution from 1 and 4 earthquakes with magnitudes M_W 3.5 and M_W 4.0, respectively, are shown, demonstrates the average impact of these Hainaut events. By computing the median and 84th percentile (84pct) distance for each damaging intensity unit, we conclude that for a M_W 3.5 event at 2.3 km depth in Hainaut, negligible to slight damage (starting from I = V) can be expected up to an epicentral distance of 3 km (84pct: 4 km). For M_W 4.0 events, substantial damage (I = 7) can occur up to a

355 median epicentral distance of 2 km (84pct: 4km); moderate damage (starting from I = VI) up to 3 km (84pct: 7 km); negligible to slight damage up to 5 km (84pct: 8 km).
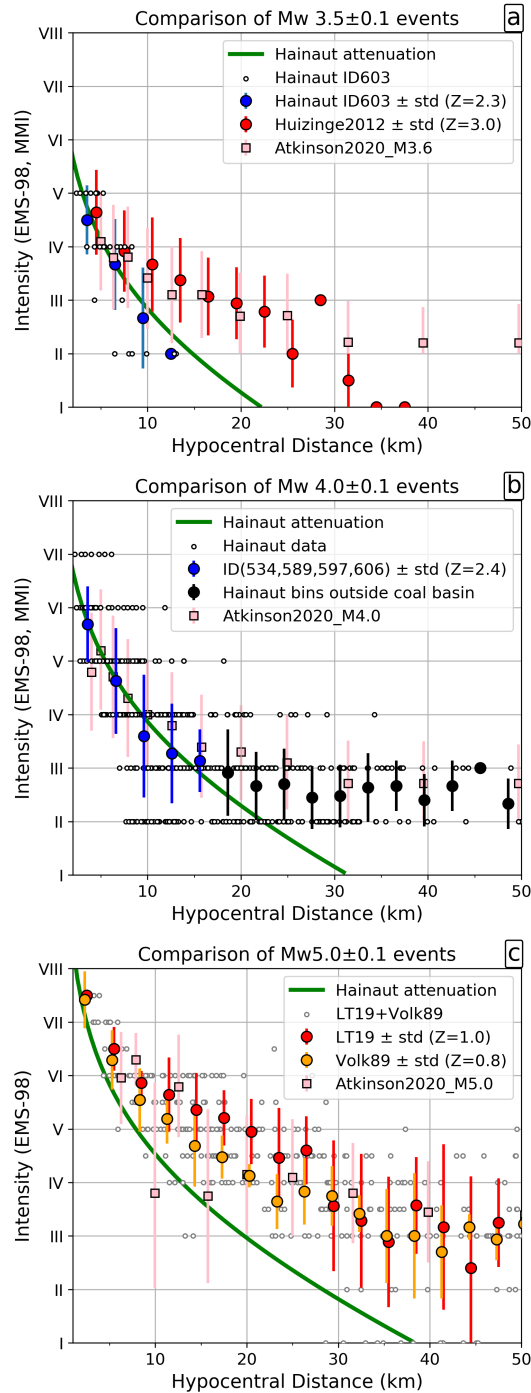
Figure 9. Comparison of binned (3 km) intensity - distance observations for a) M$_W$ 3.5 earthquakes in Hainaut, in Huizinge (Groningen gasfield, NL, Dost and Kraaijpoel, 2013), and in Oklahoma (US, Atkinson, 2020), b) M$_W$ 4.0 earthquakes in Hainaut and in Oklahoma (US), and c) M$_W$ 5.0 earthquakes in Le Teil (FR, Sira et al., 2019), Völkerhausen (DE, Leydecker et al., 1998) and Oklahoma (US). IDPs (small grey dots), mean intensity (coloured dots or squares) and standard deviation (bars) of the different intensity datasets are shown in comparison with the fast decay of the Hainaut intensity attenuation relationship (green line). Z = depth in km.
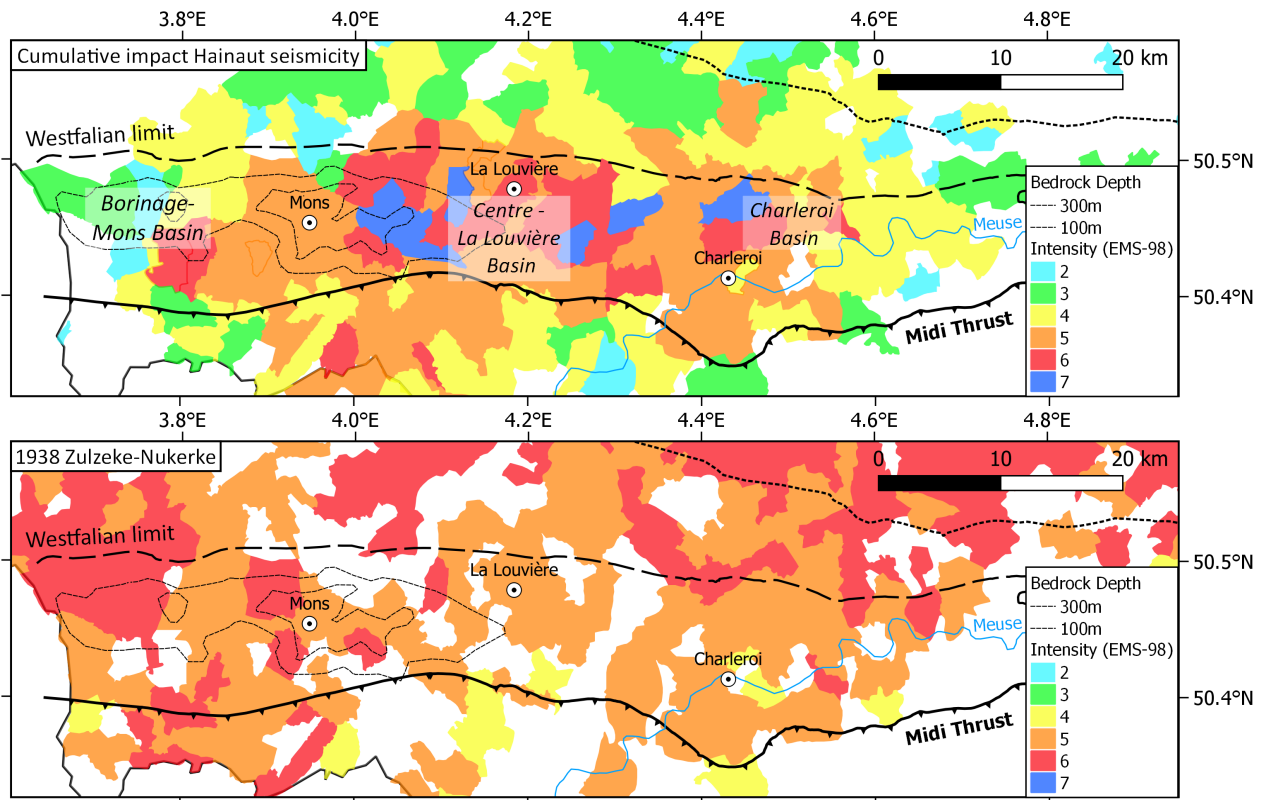
Figure 10. Top) Communal map of the Hainaut coal area showing the maximum intensities that were reached by the 124 earthquakes. Bottom) for comparison, the impact of the 1938 earthquake on the Hainaut coal area is shown. This earthquake had a larger impact on the Brabant Massif and in the western part of the Mons basin but not on the La Louvière-Centre Basin and Charleroi Basin.

To obtain a global view of the damaging character of the Hainaut seismicity, we report in Figure 10 the maximum intensity observed within each commune in the Hainaut coal area for all 124 events of the Hainaut seismic catalogue. Maximum intensity equal or greater than V was observed in all the localities in a 60 km long and 15-20 km wide range of the coal area, which extends from 10 km east of the French border to 15 km west of the city of Charleroi. Outside the coal area, this seismicity had no damaging impact and in only a few communes, intensity V was observed. The area between Mons and Charleroi and centered on La Louvière was the most affected part with a widespread repartition of maximal intensity VI, including some localities where intensity VII was observed. In the Borinage basin, intensity VI was only observed locally in a few communes in its western part. However, this maximal intensity can have been observed more than one time in some localities.

Apart from the Hainaut seismicity, also two other 20th century earthquakes had a strong local impact on the Hainaut coal area: i.e. the strongly damaging 11 June 1938 Zulzeke-Nukerke M_W=5.0 (S30) and the 20 June 1995 M_W=4.1 Le Roeulx (S31) earthquakes in the Brabant Massif (Fig. 1). Both events occurred much deeper (20 and 25 km, respectively) and had a totally different effect than the Hainaut earthquakes because they were widely felt. In many localities in the coal area, intensity

V was reported. Intensity VI was observed, mostly only in the western part. Despite that the 1938 earthquake occurred 40 to 45 km north-west of the western extremity of the Hainaut coal area, this event caused more local slight damage in the Borinage, than the maximal cumulative impact of the Hainaut seismicity (Figure 10b). Outside the coal area, the impact of the 1938 earthquake is even larger everywhere. Similar conclusions arise from the few original documents concerning the effects of historical earthquakes. Some of them had a larger impact in the coal area than the individual 19th or 20th century Hainaut earthquakes. Apart from the effects of the 23 February 1828 earthquake (see section 2), the earthquake that had the largest impact in the area is the 18 September 1692 M_W = 6.0 earthquake that occurred in the Belgian Ardennes (Fig. 1). This large earthquake caused significant damage in the city of Mons where *"many houses, churches and other buildings were damaged and half ruined and more than 80 people were either killed or injured"* (Alexandre et al., 2008). These differences in impact between the Hainaut coal area events and seismic sources outside the Hainaut area, indicate that the contribution of the Hainaut coal area seismicity to the impact of earthquake activity in southern Belgium and northern France during the last 300 years (Fig. 1) is overestimated. However, inside the coal area, we have to keep in mind that the maximal intensity was reported in some localities more than one time.

Seismic events in the Hainaut coal area often occurred in seismic sequences that sometimes lasted several weeks. The repetition of shakings and waking up during the night, and the increasing damage that sometimes led to the ruin of some houses aggravated the way this seismicity was experienced by people. This was particularly true during the Havré seismic sequence of April-May 1949. Moreover, as the population associated this seismic activity to the mining industry, it was at the origin of many complaints against this industry. To date, there is no study analysing the impact of these earthquakes on the population of the Hainaut coalfield in comparison with the numerous other nuisances created by mining. Indeed, many buildings in the Hainaut coal area were damaged due to underground progression of the coal exploitation and the progressive settling that follows. Troch (2018a, b) present the example of the locality of Gosselies near Charleroi, which was completely devastated between the two world wars because of the extensive coal production. In some areas, mine subsidence led to surfacing groundwater and increased the risk of flooding. It was necessary to evacuate the water by pumping systems otherwise wetlands, marshes, swamps, ponds and lakes appeared in the affected area (Troch, 2016). The subsidence and the permanency of humidity in some areas caused by mining activities are also factors affecting the resistance of buildings.

6.3   Intensity attenuation modelling

We assume in section 4.2 that the spatial distribution of intensity observations is adequate in number and is spatially unbiased, which allowed correctly quantifying the rapid intensity decay with epicentral distance in the coal areas. For the 12 earthquakes included in the attenuation analysis, 813 IDPs are available (Table 2). These IDPS are mainly derived from the information provided by the ROB official survey since 1949. The high population density in the coal area explains why within a radius of 15-20 km, most of the local authorities answered to the inquiry (see Fig. B1 or the Atlas). For earthquakes older than 50 years, such a density of information provides a real opportunity to study the earthquake impact because there are very few biases in azimuth and distance. Outside the coal area, the population density is lower and the areas are more rural, which could explain why local authorities took less care in answering the official inquiry and why information mainly came from the larger

localities. Of course, the largest Hainaut earthquakes were only weakly felt (intensity II to III) in these areas and the answers to the inquiry may provide an unrepresentative view of the earthquake effects. This under representation does not only occur in historical earthquake records but can also be present in online DYFI? records for some parts of the world where online data collections are not broadly accessible (Hough and Martin, 2021).

Hence, the most limiting factor in the information is the resolution of the distance between the IDPs. Before the community fusion in 1977, the size of the communes ranged between 3 and 15 km^2, with a mean equivalent circular radius ranging between 1.0 and 2.0 km. After 1977, community size and radius increased and ranges, respectively between 17 and 65 km^2 and 2.3 to 4.5 km^2. The small dimension of the communes explain why the steps considered in the intensity distance binning is 2.5 or 3 km, which are just at the limit of undersampling a range of two intensity values from the epicentre for events with a focal depth of 1 km (Fig. 6). The intensity averaging process in the communes induced by this inquiry also leads to under-estimation of peaks of intensity at local places, an unfortunate effect that is even larger for the bigger communes after the fusion. For some larger earthquakes, we could rely on press reports and letter testimonies to highlight some of these locally increased intensities and to identify where they are located. For Belgian earthquakes between 1977 and 2002, this communal resolution problem complicates intensity modelling. Fortunately, the availability of the ROB online *Did You Feel It?* inquiry since 2002 (Camelbeeck et al., 2003; Lecocq et al., 2009) can resolve this granularity in the future as street addresses of testimonies can now be geocoded and intensity data can be aggregated in size-adaptable grid cells (Van Noten et al., 2017). For potential future events, this strategy might allow oversampling the macroseismic field and modelling the intensity variability in each commune, except in localities with extensive damage (cf. the Doughnut Effect in Bossu et al., 2017) where field surveys would then be needed (as done by Sira, 2015).

Van Noten et al. (2017) and Camelbeeck et al. (2021) illustrated how regional geological structures and bedrock depth in Belgium and surrounding regions have an effect on intensity attenuation. Our gathered intensity dataset suggests that outside the Hainaut coal area, intensity attenuates similarly as indicated by these authors, i.e. a slow intensity attenuation to the north and south, within the borders of the Brabant Massif basement and the Ardennes, respectively. As our intensity evaluation is mainly based on the ROB inquiry, IDPs represent a mean intensity in each locality which hampers to sub-sample below communal dimensions. Hence, the dataset does not allow distinguishing intensity variations linked to local differences in thickness and composition of sedimentary near-surface deposits within the Hainaut coal region. The dataset certainly can be used to evidence the role of large-dimensional geological structures in Belgium on intensity attenuation (e.g. Neefs et al., 2021), but this is beyond the scope of this paper.

We now can model the attenuation of intensity in the coal mining area of Hainaut as follows:

$$I = I_0 - 3.42 * log(\sqrt{\frac{R^2 + Z^2}{Z^2}}) - 0.054 * (\sqrt{R^2 + Z^2} - Z) \tag{6}$$

with I_0 determined from the magnitude (see eqs. 3 and 5) or I_0 = Imax for earthquakes with only few IDPs, but with a clearly determined epicentral intensity. For these events, Imax scaled to the magnitude (eqs. 4 and 5) can be used for intensity modelling. Applying this attenuation formula (Fig. 3) shows that the intensity prediction works well inside the Hainaut coal area. However, the formula is not meant to predict intensities outside the coal area. Within the border of the Brabant Massif,

the e.g. 1967 Carnières event (Fig. 3) is felt farther than the intensity attenuation model predicts and a different attenuation model should be constructed.

6.4 Focal depth determination

440 Inferring focal depths from macroseismic data provides a robust and alternative way when instrumental data is lacking (Sbarra et al., 2019). Previous authors used intensity data to evaluate the focal depth of some of the largest earthquakes in Hainaut. Charlier (1949) evaluated the focal depth of the 3 April 1949 earthquake to 3.4 km, while Van Gils (1966) provided values of 6.5 km, 4.3 km and 5.0 km respectively for the earthquakes of 15 December 1965, 16 January 1966 at 6h51m and 12h33m. Ahorner (1972) estimated the focal depth of the 15 December 1965, 16 January 1966 and 28 March 1967 respectively to 2.4,
445 1.9 and 3.0 km. Even if these determinations indicate that these earthquakes occurred at shallow depth, the difference by a factor of two in the evaluated focal depths between Ahorner (1972) and Van Gils (1966) is difficult to interpret because none of these two authors provide an uncertainty on their determination and explain how they choose the attenuation parameters they used. The approach developed in this study solves these two issues (i) by evaluating attenuation parameters directly from the Hainaut intensity dataset and (ii) by providing a way to evaluate uncertainties linked to the attenuation model and the
450 intensity determination in a systematic way for all the events. Our results show that focal depth estimated by Charlier (1949) and Ahorner (1972) are inside our error bars.

The ideal test of the robustness of the macroseismic method to evaluate the focal depth of shallow earthquakes would be to compare focal depths determined by this method with the ones estimated by the classic microseismic method based on seismic phase arrival time measurements. In our dataset, the only earthquake for which focal depth was determined from arrival phase
455 measurements in seismic stations is the 8 November 1983 Liège earthquake. In their comprehensive study of the earthquake, Ahorner and Pelzing (1985) evaluated the focal depth as 6 ± 2 km. Faber and Bonjer (1985) interpreted depth phases recorded by the Gräfenberg network in Germany and concluded that a depth of 4 km would fit better the seismograms. If we use the new Hainaut attenuation model that would be similar in the Liège area, the focal depth of the Liège earthquake is 5.7 ± 1.5 km (see Table 3), which agrees well with instrumental evaluations.
460 Since 1985, it is possible to evaluate focal depth of earthquakes occurring in the Hainaut coal area by using phase arrival times of the Belgian seismic network. In Fig. 11, we compare the depth distribution of the earthquakes that occurred before and after this date to analyse and explain their similarities and (or) differences. Since 1985, 29 earthquakes have been located in the Hainaut coal area (Fig. 11a) with a depth uncertainty of less than 4 km (Fig. 11b). The largest observed magnitude between 1985 and 2020 is M_W 2.6. Despite a dense seismic network in or near the Hainaut coal area, the focal depth uncertainty still
465 remains significant with a mean value around 2 km, while our estimate of the uncertainties for earthquakes before 1985 using macroseismic data are lower than 2 km (Fig. 11b). The main reason for this difference is that the distance between earthquake epicentres and the closest seismic station is often greater than 10 km, which is not sufficient to determine focal depths of less than 4-5 km with a high precision (Gomberg et al., 1990).

The two depth distributions coincide for focal depths between 1.75 and 4 km with 24 events on a total of 41 before 1985
470 and 9 events on a total of 29 after 1985. The two distributions also present two main differences: before 1985, many events
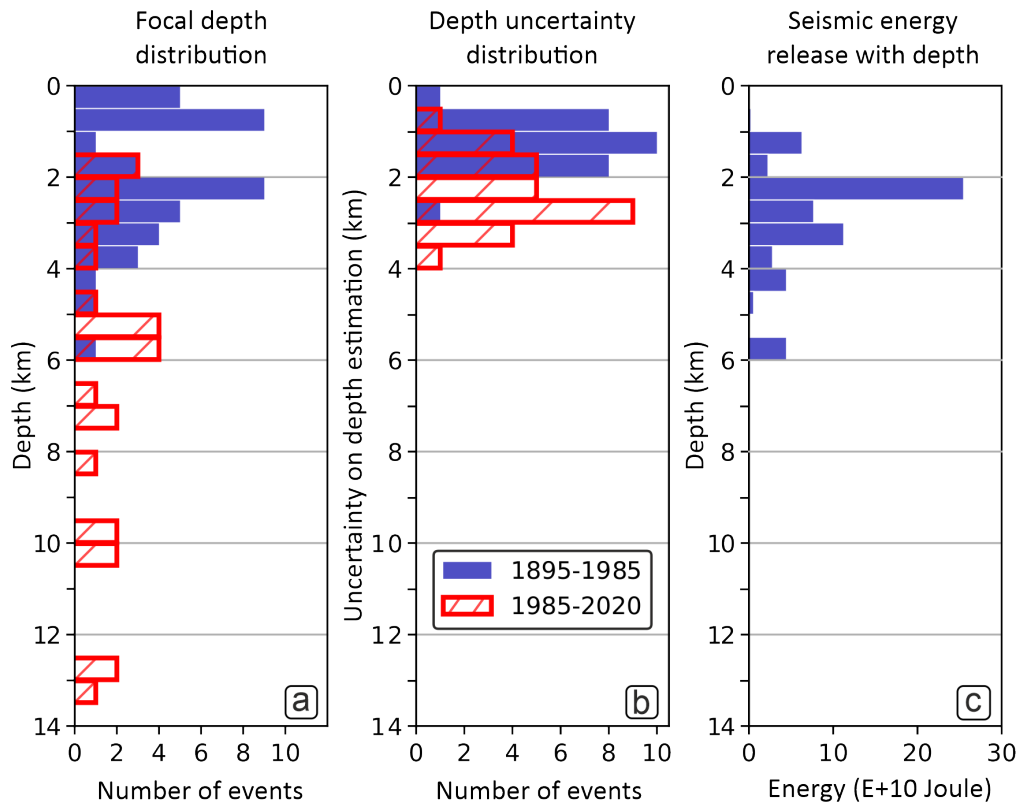
Figure 11. A) Focal depth distribution of earthquakes in Hainaut before and after 1985. For earthquakes before 1985, the estimations come from macroseismic data as explained in section 4, while after 1985 depth comes from microseismic location (source: ROB earthquake catalog). B) Distribution of the uncertainties on these focal depth determinations. C) Seismic energy release with depth.

occurred at very shallow depths of less than 1.75 km (21 events on a total of 41), versus none after 1985. Moreover, most (20 of 29) of the events after 1985 occurred at depths greater than 4.0 km, up to 13 km, while only 3 earthquakes before 1985 occurred at more than 4 km, but still less than 6 km. All the very shallow events at less than 1 km occurred before 1960, which precedes the end of the mining activities at the end of the seventies. These events contributed only little to the seismic energy

475   release in the Hainaut coal area (Fig. 11c) because even if most of them were strongly felt or caused slight damage, they were of small magnitude. This is confirmed by the fact that they were not recorded by the seismic station in Uccle (at 35 km for the most northern Hainaut event). Their location inside the coal mining area, their period of occurrence, their very shallow depth and their weak radiated seismic energy could be indicators of a very close link to mining activities.

    The seismic activity between 2 and 4 km depth, which is below the deepest mining excavations at a little more than 1 km, can

480   not be directly associated with mining. Nevertheless, the seismic activity strongly diminished after the progressive closure of the mining industry during the seventies, after the high level of activity observed between 1965-1970. This led to the hypothesis that this part of the Hainaut seismicity could be triggered by mining activity. However, the origin of this seismicity should be

interpreted at the light of recent studies on earthquake activity in stable continental regions suggesting that it can be explained by transient disturbances of the local crustal stress or changes in fault strength (Camelbeeck et al., 2013; Calais et al., 2016).

485   Similar questions also arise for the seismic activity deeper than 5 km that has only been observed since 1985. However, the small magnitude of these events could explain that similar earthquakes could have occurred before 1985 but were not detected because they were not felt, nor recorded by any seismic station. These earthquakes could be a background of natural seismicity, but also a seismicity indirectly triggered by the past mining industry. These issues will need to be studied using more quantitative data on stress modifications caused by mining exploitation in the upper crust, time and spatial evolution of

490   the observed seismicity, earthquake fault-plane solutions, and better interpretation of the surrounding seismotectonic context.

7   Conclusions

Our study provides a comprehensive overview of the earthquake activity in the Hainaut coal area and discusses its impact from the end of the 19th century up to 1985, when the implementation of a modern digital seismic network began in Belgium. We updated the ROB earthquake catalogue for magnitude, depth and maximal observed intensity. We also present a digital archive

495   describing the effects of these earthquakes. We re-evaluated the local intensities of the well-documented earthquakes from these records. They are all included in the Supplement attached to this paper. Our earthquake analysis and impact estimation underline the severity of the damage locally caused by the strongest earthquakes in Hainaut. For earthquakes in the M_W magnitude range between 3.5 and 4.0, maximal observed intensity reaches VI or VII in the EMS-98 macroseismic scale.

    Our analysis suggests that the contribution of the Hainaut coal area seismicity on current seismic hazard maps in Belgium

500   and northern France (Fig. 1) are overestimated and need re-evaluation, on the one hand because the magnitude of the largest events have been downsized in our new catalogue and, on the other hand, because the seismic energy is rapidly absorbed within the fractured Hainaut coal basin due to the strong attenuation. This conclusion provides new perspectives for seismic hazard issues in Hainaut. First, it demonstrates the importance of using more appropriate GMPEs for the Hainaut area that are in line with the observed rapid intensity decay with distance than the current used GMPEs. The presented intensity dataset will

505   help to identify the most adequate GMPE. Second, the potential causality between the coal mining extraction that ended in the 1970s and the Hainaut seismicity can now be studied using the new reliable focal depths estimated from the IDP distributions. Finally, the damaging character and the fast intensity attenuation of shallow Hainaut events should be included in the impact and ground motion modelling of potential induced seismicity related to current and future deep geothermal projects in the area.

Appendix A: Intensity evaluation

510   **A1   Background to evaluate intensity**

An optimal dataset to evaluate intensity would be the one describing the way many people in each locality felt an earthquake inside its perceptibility area and furnishing the specific degree of damage for each building hit by the event. This can be obtained when a specific inquiry is dedicated to collect such a large amount of information. This level of quality is obtained by

the ROB online *Did You Feel It?* inquiry since 2002 (Camelbeeck et al., 2003; Lecocq et al., 2009), but up to now, it concerned earthquakes where mean maximal intensity did not reach intensity V in any locality. For intensities equal or larger than V, such an extensive dataset only exists for the destructive 8 November 1983 M_W=4.6 Liège earthquake in east Belgium, but this is an exceptional case in NW Europe. This precise damage information came from the owners of 17,000 buildings that sent detailed damage reports of their property, which was evaluated by the Belgian Federal Calamity Centre in order to reimburse the repair costs. These data were at the base of seismic risk studies on the Liège area (Jongmans and Plumier, 2000; Garcia Moreno and Camelbeeck, 2013; Camelbeeck et al., 2014).

The ROB survey and some of the scientific studies described in section 3.1 are not so detailed, but they furnish information to evaluate intensity at the scale of each locality and have the advantage to sample the complete macroseismic field of the studied earthquakes. Information in the press does not sample the whole area of perceptibility and is often concentrated on the most visible effects of the earthquakes. We determine intensity in the following way: when the answers to the questions in the ROB questionnaire and (or) information from other sources fulfil and exceed the EMS-98 description of the earthquake effects at a given intensity degree I, but are not compatible to the description corresponding to a higher intensity value I+1, the intensity is fixed to the single integer value I. When the observations do not allow discriminating between two intensity values, a range of corresponding intensity values is given. Information coming from some localities for earthquakes that were not the object of an official survey is sometimes insufficient to assess intensity although the seismic event was reported as felt. We indicated these places with an "F" on the macroseismic maps. When the answers to the ROB official survey in one locality were all negative (see inquiry books in the Supplement), we considered the earthquake as not felt there, but we do not report this information on the macroseismic maps as the consulted sources are insufficient to establish the limit of perceptibility.

A2 Building vulnerability

For intensity greater or equal to V, a significant part of our evaluations comes from damage observations. To assess intensity, it is necessary to know the building stock and vulnerability class distribution in the studied area from the beginning of the 20th century to around 1970. At the exception of Barszez (2005), who studied the seismic vulnerability of historical houses in the centre of the Mons, there is no study analyzing the seismic resistance of buildings in the Hainaut coal area. Fortunately, the building stock is relatively similar to the one in the Liège region that was well studied after the 1983 Liège earthquake (Garcia Moreno and Camelbeeck, 2013; Phillips, 1985; Plumier, 1985, 2007). The main reason for this resemblance is that the two regions experienced a similar rapid population expansion due to strong industrial development that accompanied the extensive exploitation of coal and development of an important steel industry. Unreinforced masonry houses formed an important part of the building stock, which was common in this part of Europe during the 20th century. This type of building is associated with vulnerability class B in the EMS-98, but it can range between class A for the most vulnerable and class C for the least vulnerable buildings according to the quality of their foundation, construction and maintenance. During the 1983 Liège earthquake, part of these masonry buildings showed deficiencies which were at the origin of serious structural damage. The most affected structures were unreinforced low-rise masonry dwellings for which the links of the floors and the load-bearing walls were weak or even missing. Many of those buildings shared walls with the neighboring houses (Phillips, 1985;

Plumier, 1985, 2007). The importance of the damage on these buildings compared to the better behaviour of well-constructed brick buildings clearly suggest that they belong to class A in the EMS-98 classification. In the Hainaut coal area, the same type of buildings are represented in many corons where families of workers in the mining and siderurgy industries are living. However, many buildings also suffered from damage directly associated with mining activities including the underground progression of coal exploitation and the progressive settling that follows (see discussion). Increased humidity due to surfacing groundwater and pre-existing structural weaknesses associated with mining activities increased the vulnerability of buildings. These aggravating circumstances suggest that a significant part, which is unfortunately undetermined, of the building stock are to be classified in the class A vulnerability defined in the EMS-98 macroseismic scale.

A3 Intensity from damage

In the ROB questionnaire, questions concerning damage to buildings allow fixing intensity equal to or greater than V (see inquiry books). The observation of small fragments of plasters that fell from the ceilings and of broken or cracked windows appear at intensity V. EMS-98 considers brick chimneys behaviour as representative of the damage grade on masonry buildings because it is the most visible manifestation of the seismic action during moderate earthquakes. Indeed, fireplaces are slender objects, not very resistant to bending, especially since the corrosion of the mortar transforms them into a pile of bricks stacked without much connection (Plumier, 1985). Their partial collapse is an indicator of damage grade 2 (moderate), while fracture at the roof junction corresponds to grade 3 (sensitive to severe damage). The last question in the form asks the local authorities about the number of damaged and overturned chimneys, which theoretically allows the seismologist to evaluate the percentage of grades 2 and 3 damage in the locality. Considering that the most important damage occurred on the most vulnerable part of the masonry buildings, the quantity of fallen/damaged chimneys provides a way to either confirm intensity V (very few damaged chimneys) or help discriminating between intensity VI and VII if, respectively, few or many chimneys were overturned. The EMS-98 scale defines the limit between the quantities "few" and "many" as being between 10% and 20% of the number of considered buildings in a specific vulnerability class. Then, the percentage of building vulnerability class A in a locality is an important factor in the intensity evaluation process. Unfortunately, this information is lacking and we are forced to make simplistic assumptions about it. Here, we considered that half of the buildings are in class A and that only these most vulnerable structures suffered the highest observed damage grade. This means that the observation of 5% or more of overturned chimneys in a locality would correspond to 10% or more of grade 3 damage on vulnerability class A buildings, which corresponds to intensity VII. Of course, grade 2 damage should also be observed in many buildings of class B and class A. We considered that simultaneous observation of 5% grade 3 and 5% grade 2 damage would be associated with intensity VII. When both of these percentages of damage are smaller than 5%, we assign intensity as VI if they are greater than 1% and V if they are smaller. The official survey also asks for the observation of large and extensive cracks in walls. A positive answer to this question indicates damage grade 3, but as the question does not ask for any quantification, it is not possible to fix the intensity to VI or VII based on this information.

At intensity VII, reports should mention serious failure of walls and partial structural failure of roofs and floors, corresponding to grade 4 damage, in few buildings of class A. Unfortunately, the ROB questionnaire does not allow to identify the

importance of cracks in walls and building structural damage. Assessing this kind of damage would require specific building inspections by a specialised engineer. Nevertheless, press articles provided local observations that we interpreted as grade 4 damage and can be used to confirm the estimated intensity of VII in some localities.

585 **Appendix B: Description of the strongest, often damaging, Hainaut earthquakes**

In this appendix, we chronologically present information on the earthquakes that were widely felt or caused damage in the Hainaut coal area (reported in Table 1).

B1   The March-June 1911 Ransart – Gosselies seismic sequence

The first known earthquake that caused damage in the Hainaut coal area occurred at 0h05m on 29 March 1911 north of the
590 city of Charleroi. A violent tremor accompanied by a tremendous noise awakened the population of the communes of Ransart, Gosselies, Heppignies and Wayaux. It shook the houses for a few seconds, enough to knock over furniture, break dishes, open unlocked doors and frighten people. However, because the earthquake occurred at night, there were no testimonies for the newspapers to report from which intensities II to IV can be evaluated. Hence, newspapers only reported information in a radius of 3 to 4 km where people awaked by the earthquake effect. In Ransart, many cracks in houses were reported and the school
595 chimney was knocked over. The magnitude of this seismic event is estimated to M_W=3.5 from the seismic recordings at the Uccle seismic station located nearly 40 km north of the assumed epicentre. After this earthquake, some light tremors occurred on 12 April 1911 (Fig. S1), in the region of Mons and Cuesmes on the other side of the coal mining area.

Two months later, the earth shook again north of Charleroi, but more strongly with a M_W=3.9 event on 1 June at 22h51m (Figs. B1 and S2) and a M_W=4.0 event on 3 June at 14h35m (Fig. S3). The epicentral area of the 1 June 1911 earthquake
600 includes the localities of Gosselies, Lambusart and Ransart where the tremors were violent enough to awaken most of the inhabitants, knocking down many chimneys and causing cracks in the least resistant buildings (Cambier, 1911). According to newspapers *"Le courrier de l'Escaut – 4/6/1911"* and *"La Meuse – 3/6/1911"* the most affected locality was Ransart where more or less 50 chimneys collapsed and a parked mine train was derailed from the tracks. A wire-drawing factory would have collapsed in Gosselies, killing 1 person and injuring 3 others. We assessed intensity to VI in Ransart, Gosselies and Lambusart.
605 In the neighboring localities of Roux and Courcelles, the visible damage was limited to a few smokestacks that were knocked down (intensity V-VI).

Curiously, Cambier (1911) did not provide any information on the 3 June 1911 earthquake, which was more damaging than the 1 June 1911 earthquake as reported by the newspapers. In Gosselies, there were entire streets where almost all the chimneys were knocked over, damaging roofs and skylights. In the houses, objects hanging from the walls were thrown to the
610 ground (*"Journal de Bruxelles – 5/6/1911"*). *"La Gazette de Charleroi – 4/6/1911"* mentions that many houses are cracked and windows are broken, and the damage would be more concentrated near the Gosselies station. The importance of the damage led us to estimate intensity to VII in Gosselies. Newspapers also describe damage in Ransart, but they are less important than
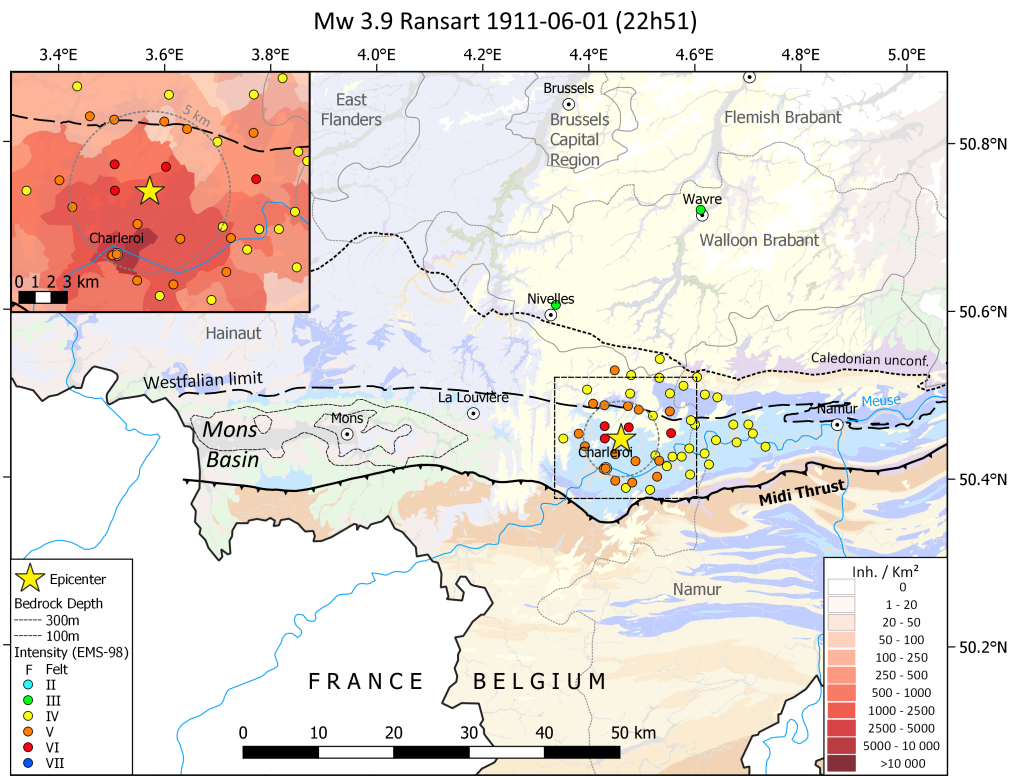
Figure B1. Macroseismic map of the 1 June 1911 M$_W$=3.9 (M$_L$=4.2) Ransart earthquake (nr 2 in Table 1). Maximal intensity = VI. Geology in background based upon http://www.onegeology.org/. Reproduced with the permission of OneGeology. All rights Reserved. The inlet shows the population density.

during the 1 June 1911 earthquake. The damage repartition clearly suggests that the earthquake of 3 June would be located in Gosselies, 2-3 km to the northwest of the epicentre of the 1 June seismic event in Ransart.

B2   The 17 January 1920 earthquake in the Borinage

This M$_W$=3.5 earthquake (Fig. S4) recorded by the seismic station of Uccle occurred at 3h11m in the morning. The newspapers report that falling chimneys tore off rooftiles in Boussu and Hornu. In the miners' houses, objects collided with each other, were moved or knocked over. Capiau (1920) published a brief notice of his observations on the earthquake effects. Maximum intensity is set to VI based on these newspaper reports.

B3   The 9 May 1931 earthquake east of La Louvière

This M$_W$=3.0 event is a smaller event than the previous ones. In the epicentral area, many residents rushed outside while in some neighbourhoods the doors of the houses opened. A chimney collapsed in Houdeng-Aimeries (Fig. S5).

B4 The 5 November 1936 Trazegnies-Chapelle earthquake

This M_W=3.3 earthquake (Fig. S6) did not cause any damage but many inhabitants of the communes of Trazegnies, Piéton, Gouvy-Lez-Piéton, Godarville and Chapelle were awakened by the shakings. The main observations are that windows vibrated while small objects were knocked over from shelving furniture and fireplaces (*"L'Indépendance Belge - 7/11/1936"*).

B5 The 7 and 9 January 1940 earthquakes east of La Louvière

Three small events recorded by the Uccle seismic station occurred in January 1940 near La Louvière (Figs. S7, S8, S9). The first of M_W=3.5 on 7 January at 16h28m was best recorded in Uccle and was the most violent of the sequence. In La Louvière, furniture was moved while vases placed on the marbles of the fireplaces as well as doors and windows shook. The newspaper "La Gazette de Charleroi" shows a photo of a damaged fireplace in Saint-Vaast indicating that slight damage was observed. The two earthquakes that followed were more weakly felt. The 9 January 1940 earthquake (M_W=3.1) that occurred early in the morning woke up few people but has been locally felt by workers in the coal mines near La Louvière (Fig. S9).

B6 The 3 and 14 April 1949 Havré-Boussoit earthquakes

One of the strongest earthquakes in the Hainaut coal area occurred on 3 April 1949 at 12h33m in the region of Havré, 8 km to the east of Mons. This M_W=4.1 earthquake was preceded at 12h27m by a M_W=3.7 event, which was also strongly felt. The ROB conducted a detailed survey about the damage and effects caused by the 12h33 earthquake (Charlier, 1951). This earthquake is the first one for which the ROB organised an official survey on a large part of the Belgian territory. The macroseismic map based on our reassessment of intensities in the EMS-98 macroseismic scale are reported on Figures 4 and S10. The most affected localities are Boussoit, Havré and Maurage where we estimate intensity to VII. In Havré, there was a beginning of panic after the 12h33 tremor, which was so violent that more than 80% of the chimneys out of 1400 dwellings were disrupted, of which 50% needed to be completely rebuilt, and 150 had been completely overturned. In Boussoit, at least 70% of the chimneys were damaged or collapsed, while in Maurage about 200 and 25 chimneys were respectively damaged and overturned. In Maurage, the vault of the church choir was damaged by a crack while in Trivières, a slag heap has collapsed, endangering the neighbouring dwellings. The earthquake was followed by a number of aftershocks that were felt in the epicentral area. Only few of them were recorded at the Uccle seismic station and (or) reported in newspapers with sufficient precision to be classified in a list. 11 days after the mainshock, on 14 April 1949 at 01h09 (Fig. S11) and 05h12 (Fig. S12), the earth shook again in Havré with magnitudes of M_W=3.5 and M_W=3.6. The macroseismic data coverage for these events is poor, but still a maximum intensity of respectively V and VI has been reported.

B7 The October 1952 earthquake sequence in the Borinage

In October 1952, three earthquakes shook the Borinage area west of Mons. The first two occurred on 21 and 22 October (M_W=3.1 and M_W=2.8; Figs. S13 and S14), respectively at 21h15m and around 7h, and were moderately felt by the people. The third earthquake on 27 October 1952 at 6h11m (M_W=3.5; Fig. S15) was stronger and caused uproar among a part of the
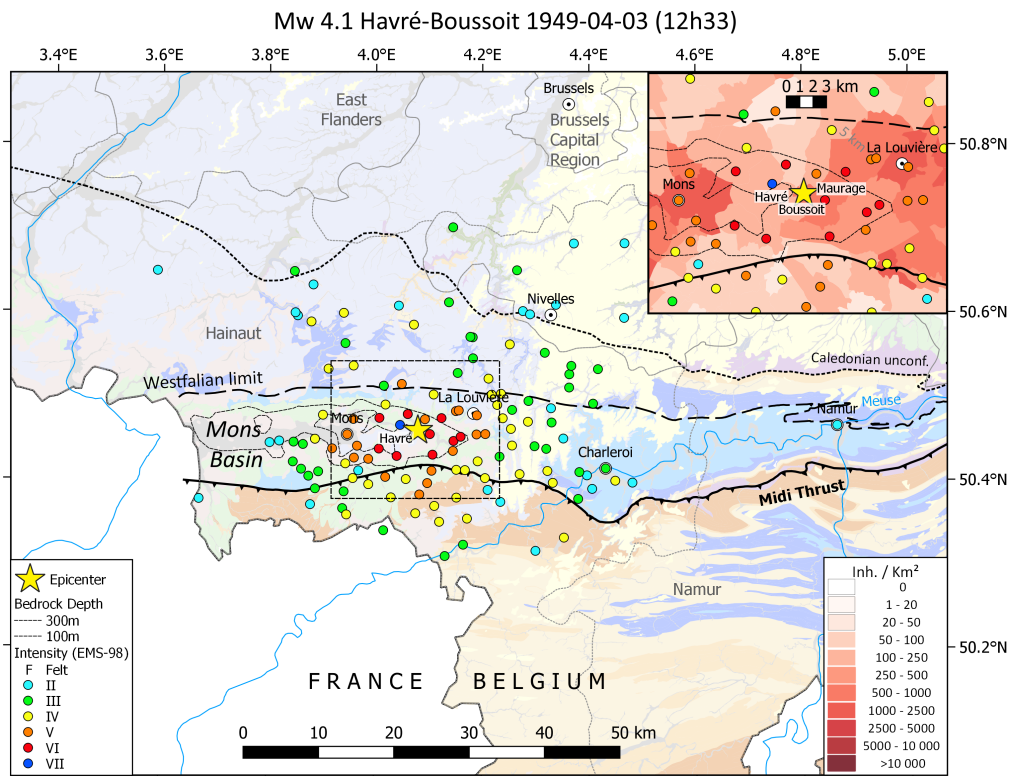
Figure B2. Macroseismic map of the 3 April 1949 M_W=4.1 (M_L=4.6) earthquake in the Borinage (nr 10 in Table 1). Maximal intensity = VII. Geology in background based upon http://www.onegeology.org/. Reproduced with the permission of OneGeology. All rights Reserved. The inlet shows the population density.

population who rushed out of the dwellings in the localities of Cuesmes, Flénu, Hornu, Jemappes, Quaregnon and Wasmes. 655 The damage was limited to pieces of plaster falling from the ceilings, falling bricks, and falling pieces of chimneys in poor condition (intensity V).

B8 The 10 July 1954 earthquake in the Borinage

On 10 July 1954 at 17h18m, another earthquake (M_W=3.5; Figs. B3 and S16) shook the same area than the 1952 events, with consequences relatively similar to those observed during the 27 October 1952 event. The local authorities paid much attention 660 to properly filling the ROB official survey and indicated precise numbers on the damage to chimneys, indicating a slightly larger damage. We estimated intensity to V-VI in the localities of Quaregnon and Ghlin where the earthquake damaged 25 and 7 chimneys, respectively.
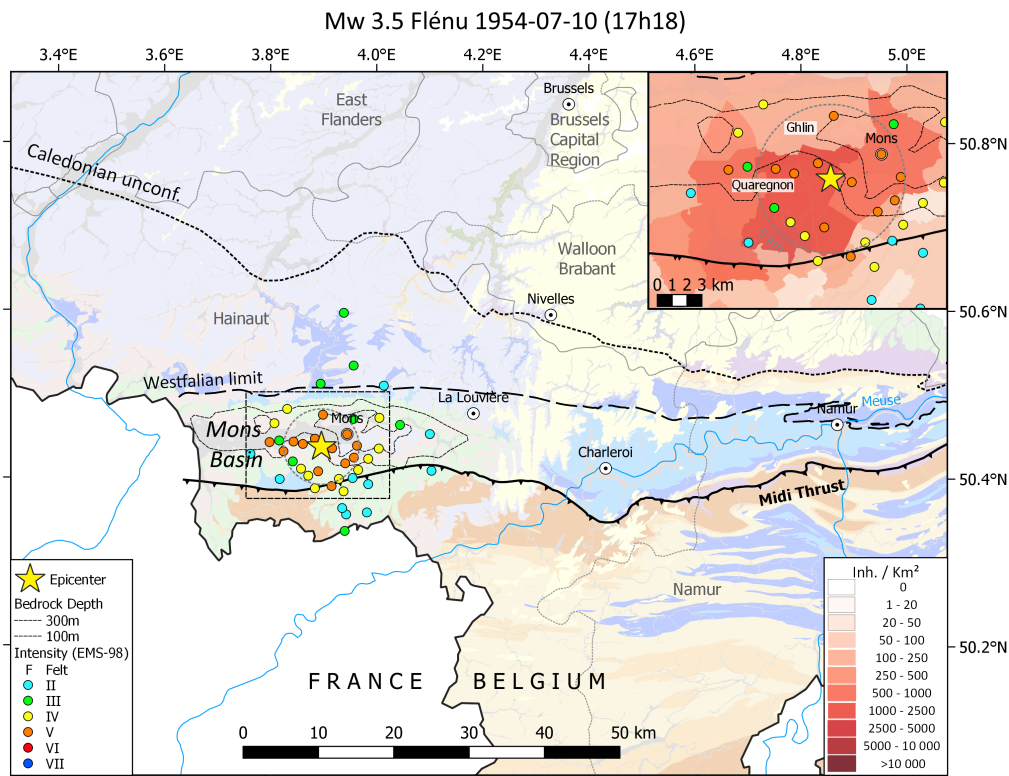
Figure B3. Macroseismic map of the 1954 M_W=3.5 earthquake in the Borinage (nr 16 in Table 1). Maximal intensity = V. Geology in background based upon http://www.onegeology.org/. Reproduced with the permission of OneGeology. All rights Reserved. The inlet shows the population density.

B9   The 15 December 1965 earthquake near Strépy-Bracquegnies

On 15 December 1965 at 12h07m, a violent M_W=4.0 earthquake (Figs. B4 and S17) that lasted several seconds shook the region west of La Louvière and caused considerable commotion throughout the region (*"L'Indépendance (Edition du Centre) - 16/12/1965"*). There was quite some damage, especially to chimneys and roofs, but also to verandas damaged by falling chimneys. Few casualties occurred as people were hit by pieces of glass from shattered windows or skylights. The damage was the most important in Strépy-Bracquegnies. In this locality, there were overturned chimneys in practically every street, cracks in several buildings and many broken windows. Fallen stones and bricks damaged several cars. The ROB official questionnaire mentions 230 damaged and 122 overturned chimneys, which corresponds to 10% of the dwellings in the locality. The reported percentage is similar in the neighbouring commune of Bray. For these two localities, we assessed intensity as VII in EMS-98. We evaluated intensity as VI in Maurage and Trivières where the earthquake caused deep cracks in bricks and concrete walls in some houses, and damaged or overturned chimneys in 2 to 3%, respectively, of the total number of habitations. In Trivières, vials were falling off the shelves in a pharmacy, while someone had to hold the bottles of wine that were falling from the
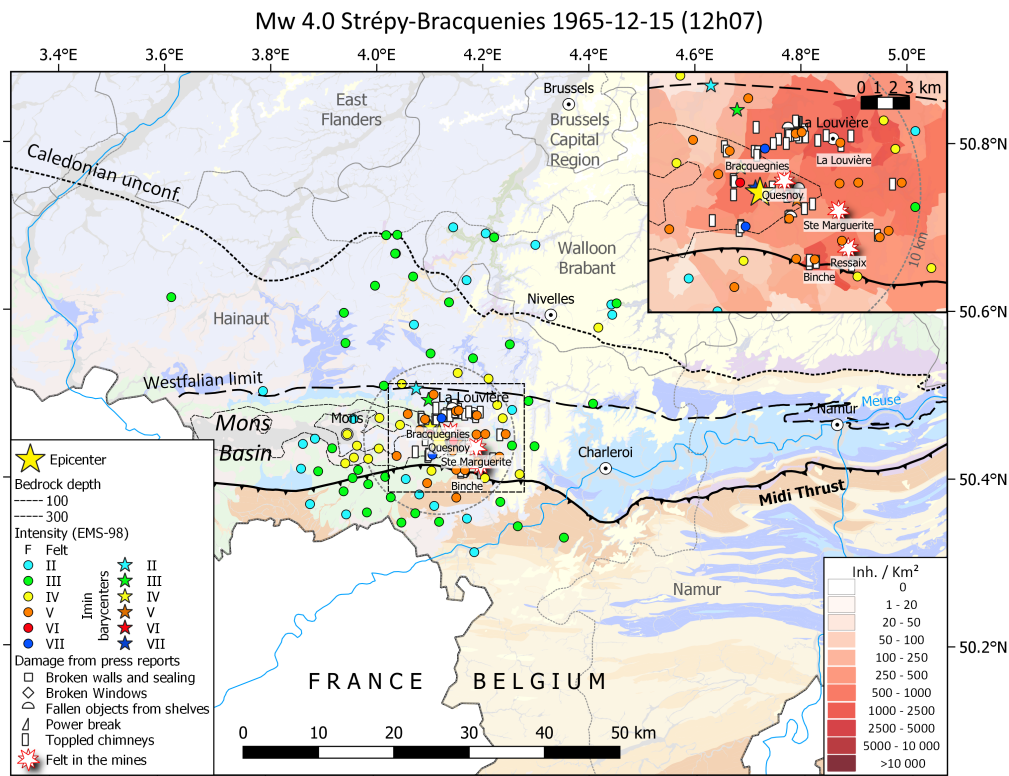
Figure B4. Macroseismic map of the 1965 M_W=4.0 (M_L=4.4) Strépy-Bracquegnies earthquake (nr 17 in Table 1). Maximal intensity = VII. Geology in background based upon http://www.onegeology.org/. Reproduced with the permission of OneGeology. All rights Reserved. The inlet shows localities where damage has been reported in press reports with population density as background.

675 shelves in a store. Minor damage was observed in surrounding localities of Binche, Boussoit, Estinnes-au-Mont, Haine-Saint-Paul, Haine-Saint-Pierre, Houdeng-Aimeries, Houdeng-Goegnies, La Louvière, Leval-Trahegnies, Le Roeulx, Mont-sainte-Aldegonde, Morlanwelz-Mariemont, Péronnes-lez-Binche, Ressaix, Thieu, Vellereille-les-Brayeux, Villers-Saint-Ghislain and Waudrez.

Miners working in the region's collieries also perceived the earthquake. This was the case at the Quesnoy collieries in
680 Trivières and at floors 872 and 1025 of the St-Marguerite coal mine in Péronnes-lez-Binche (see inlet in Fig. S17). The farthest locations from the epicentre where the ROB retrieved mentions of the earthquake were Wauthier-Braine (29 km) to the north, Viesville (21 km) to the east, Forge-Philippe (55 km) to the south, and Grandmetz (40 km) to the north-west. Remarkably, also the city of Ghent replied to the survey (73 km). The earthquake was followed the same day by three felt aftershocks.

B10 The 16 January 1966 earthquakes in the La Louvière-Centre Basin

One month after the earthquakes in Strépy-Bracquegnies, the earth shook the region a few km more to the East. On 16 January 1966, two earthquakes occurred in the morning, the first one with M_W=2.9 at 0h13m (1h13m local time; Fig. S18) and the second one of M_W=3.5 at 6h51m (7h51m local time; Fig. S19) near Morlanwelz-Mariemont. The first seismic event woke up part of the population in La Louvière and nearby localities. The second earthquake was stronger and caused damage to few chimneys and the falling plaster inside few houses in the locality of Haine-Saint-Pierre (intensity V), while it was largely felt in the localities of La Louvière, Chapelle-lez-Herlaimont, La Hestre, Jolimont, Haine-Saint-Paul and Manage.

These two events preceded a M_W=4.0 earthquake (Fig. S20) that occurred at 12h32m and caused a great deal of emotion and, in some places, even panic among the population. Indeed, in addition to minor incidents, such as falling frames, untimely clattering of glasses, vases and broken dishes, there were other more serious accidents. In Chapelle-lez-Herlaimont, Carnières, Morlanwelz, the material damage is quite considerable, although not very spectacular but, fortunately, there were no accidents to persons. Throughout the affected region, the tremor also caused a power failure and electricity only restored after ten minutes to an hour (*"Le Rappel" - 17/01/1966*). The official ROB inquiry indicates that the shock damaged or overturned more or less 400 chimneys in Carnières, which corresponds to 14% of their total number in the locality. In Morlanwelz-Mariemont this percentage is smaller, around 7-8%. We assessed intensity as VII in these two localities. In Chapelle-lez-Herlaimont and Bellecourt, we evaluated intensity as VI based on the percentage of damaged and overturned chimneys, which is nearly 3%. Minor damages are reported in La Louvière, Haine-Saint-Pierre, La Hestre, Fayt-Lez-Manage, Manage, Piéton, Souvret and Trazegnies (intensity V).

The earthquake was felt farther to the north (up to 52 km), than to the south (up to 17 km). The northwards shift of the intensity II barycentre with respect to the epicentre shows that this event was farther felt in the borders of the Brabant Massif than in the coal mining area east and west or in the Ardennes to the south.

B11 The 28 March 1967 15h49m earthquake in the La Louvière-Centre Basin

This M_W=4.1 earthquake (Figs. 3 and S21) is the strongest earthquake that occurred in the Hainaut coal area, with a similar magnitude than the 1949 Havré earthquake. The shaking was of particular violence in the region between La Louvière and Charleroi. The paper *"La Nouvelle gazette"* of 29/03/1967 reports: *"… the earthquake lasted about ten seconds, which was very frightening for a large part of the population of this region; the ground was in fact tilting underfoot and inside the buildings it seemed that the walls would not be able to resist the telluric movement. In some places, the power was cut off abruptly. Frightened, some inhabitants rushed out of their homes, while others sought refuge in their cellars."*

The most affected localities are Carnières, Morlanwelz-Mariemont and Trazegnies where the percentage of damaged or completely destroyed chimneys range from 8 to 10% (intensity VII). Inside many houses, ceilings and walls were also cracked. Fortunately, there were no personal accidents. However, emotion was very strong everywhere. In Fontaine-l'Evêque, Piéton, Chapelle-lez-Herlaimont, La Hestre and Godarville where damage is smaller, we evaluated intensity to VI.

The farthest locations from the epicentre where we retrieve mentions of the earthquake are Forest (39 km) to the north, Bonneville (54 km) to the east, Gozée (15 km) to the south, and Ville-sur-Haine (16 km) to the west. The barycentres of intensities IV, III and II are shifted northwards, showing the low attenuation properties of the Brabant Massif (Fig. 3). The earthquake was followed by many aftershocks recorded at the seismic station of Dourbes (Camelbeeck, 1985; 1993). One of these events of magnitude M_L=3.3 occurred on April 4 at 18h04. It was felt by the inhabitants of La Louvière, Carnieres and Morlanwelz but did not cause any damage.

B12   The August and September 1968 earthquakes near La Louvière

Another series of (damaging) earthquakes occurred in the summer and fall of 1968 near La Louvière. The sequence began at 7h26m on 12 August 1968 (Fig. S22) with a M_W=3.6 earthquake causing panic of people that rushed on the threshold of the houses. The ROB official survey mentions a few damaged chimneys in La Louvière, Haine-Saint-Pierre, Haine-Saint-Paul and Morlanwelz-Mariemont, which suggests that intensity could have reached V in these localities.

On August 13, a first quite violent shock of M_W=3.6 occurred at 16h17m and shook the locality of La Louvière, with a slight extension in Haine-Saint-Pierre and Haine-Saint-Paul. The rumble was brief and spectacular manifestations were limited. This event was followed by a lighter, barely perceptible tremor of M_W=3.0 at 16h40m.

The M_W=3.9 earthquake of 16h57m (Fig. S23) was stronger and damaging. In La Louvière, there was a brief moment of panic at the time of the tremor. The facades of houses vibrated, chimneys collapsed and in the workbenches of some shops, there was upheaval. The localities of Haine-Saint-Pierre and Haine-Saint-Paul also suffered from the earthquake. Chimneys fell down everywhere, but fortunately, there were no injuries. A consequence was also that all the telephone switchboards of the fire departments of La Louvière and Morlanwelz were overwhelmed (*"L'Indépendance (Edition du Centre) - 14-15/08/1968"*). Even if the number of damaged and overturned chimneys exceeded a few hundred in La Louvière, Haine-Saint-Pierre and Morlanwelz-Mariemont, this damage concerns the most inhabited part of the area and it only corresponds to a few percent of the dwellings. Hence, we estimated intensity as VI in those localities.

During the next period of approximately two months, the seismic station in Dourbes recorded a series of earthquakes. Two of them were felt in the La Louvière area and occurred on 23 September at 4h08m (M_W=3.2; Fig. S24) and 5h47m (M_W=3.0: Fig. S25).

B13   The 3 November 1970 earthquake near Charleroi

This M_W=3.6 earthquake (Fig. S26) was strongly felt and caused slight damage in the cities of Dampremy, Marchienne-au-Pont, Marcinelle, Monceau-sur-Sambre and Mont-sur-Marchienne located south of Charleroi. Many people left their homes. Damage is limited to cracks in plastered walls, small plaster fragments falling from the ceilings, cracked or broken windows, bricks falling, or few falling chimneys that were in bad condition. We assessed intensity as V in those localities.

B14   The 24 October 1976 earthquake south of the coal area

This M_W=3.9 earthquake (Fig. S27) occurred a few km south of the coal area. It strongly shook villages near the Belgian-France border. No damage was reported. The BCSF [Bureau Central Sismologique Français] conducted an inquiry on the effects of this event in France (BCSF, 1983). We used their intensity evaluations to extend macroseismic information on the French territory.

B15   The 14 September 1982, 4 and 9 August 1983 earthquakes south of the coal area

The last earthquake in the Hainaut coal area for which it was possible to provide a macroseismic map occurred near Carnières on 14 September 1982 at 19h24 (M_W=3.4; Fig. S28). Two earthquakes were also widely felt in the region of Charleroi on 4 and 9 August 1983, but only few testimonies on their effects and very few positive answers to the ROB surveys were collected.

Code availability. Codes are available from the authors upon request.

Data availability. Earthquakes that occurred in Hainaut are included in the entire earthquake catalogue maintained by the Royal Observatory of Belgium (ROB) and which can be consulted online at http://seismologie.be/en/seismology/seismicity-in-belgium/online-database

Supplement. The supplement related to this article is available online at https://doi.org/10.5194/se-0-1-2021-supplement The supplement includes:

- Table S1: The Hainaut earthquake catalogue provided as csv file (124 events)
- The Hainaut Intensity Atlas which presents
    - the Hainaut seismicity catalogue (124 events);
    - 31 intensity maps of 28 Hainaut events and 3 additional earthquakes that had a large impact on the Hainaut coal area;
    - 12 intensity-distance modelling graphs;
    - Sources and references for the entire catalogue
- 28 csv files containing intensity data of the earthquakes mapped in the Atlas
- Forms of each municipality that replied to the official surveys of the Royal Observatory of Belgium. For 17 earthquakes, an intensity inquiry book is made available in pdf.

Author contributions. TC conceptualised the research, constructed the earthquake catalogue, evaluated local intensities and executed the intensity attenuation, focal depth and magnitude modelling. TC and MH searched for historical texts in press reports. KVN produced the

(intensity) maps and the Atlas. TL computed and summarised the official ROB intensity surveys. TL and KVN calculated the cumulative Hainaut impact. TC, KVN and TL wrote the paper. All authors approved the final paper.

Competing interests. The authors declare that they have no conflict of interest.

Acknowledgements. We thank Pierre Alexandre, David Kusman and Rita Leroy for their search of documents concerning the earthquake
775   activity in the Hainaut coal area. Also thanks to Diethelm Kaiser for providing us information on mining-induced seismic events in Germany. Data analysis and modelling was performed using Python, using Scipy (Virtanen et al., 2020), Numpy (Oliphant, 2006), Geocoder (Carriere, 2021), and Pandas (McKinney, 2017) modules. Graphs were created using MatPlotLib (Hunter, 2007). Maps and attenuation modelling were constructed using QGIS (QGIS Development Team, 2021). Population density statistics for Belgium were kindly provided by Anne Joris of Statbel (Algemene Directie Statistiek – Statistics Belgium: https://statbel.fgov.be/en). The geological background in Figs. 1, 2 and 3 and in
780   all macroseismic maps in the Supplement origin from http://www.onegeology.org/. Reproduced with the permission of the OneGeology. All rights Reserved. Newspaper images shown in the supplement are free of copyright according to https://www.kbr.be/en/digitisation/digital-collections-what-about-copyrights/.

Financial support. This research was supported by funding of the Royal Observatory of Belgium.

References

Ahorner, L.: Erdbebenchronik für die Rheinlande 1964-70, Decheniana, 125, 259–283, 1972.

Ahorner, L. and Pelzing, R.: The Source Characteristics of the Liège Earthquake on November 8, 1983, From Digital Recordings in West Germany, in: Seismic activity in western Europe, pp. 263–289, D. Reidel Publishing Company 1985, 1985.

Alexandre, P., Kusman, D., and Camelbeeck, T.: La presse périodique, une source pour l'histoire des tremblements de terre dans l'espace belge, Arch Bibl Belg, 78, 257–278, 2007.

Alexandre, P., Kusman, D., Petermans, T., and Camelbeeck, T.: The 18 September 1692 Earthquake in the Belgian Ardenne and Its Aftershocks, vol. 2, pp. 209–230, Springer Science+Business Media B.V., https://doi.org/10.1007/978-1-4020-8222-1_10, 2008.

Ambraseys, N.: Intensity-attenuation and magnitude-intensity relationships for northwest european earthquakes, Earthquake Engineering & Structural Dynamics, 13, 733–778, https://doi.org/https://doi.org/10.1002/eqe.4290130604, 1985.

Association Française de génie Parasismique: Lorca earthquake (Spain), May 11th, Spain, http://www.afps-seisme.org/eng/EARTHQUAKES/Major-earthquakes/Lorca-earthquake-2011, 2011.

Atkinson, G. M.: The Intensity of Ground Motions from Induced Earthquakes with Implications for Damage Potential, Bulletin of the Seismological Society of America, 110, 2366–2379, https://doi.org/10.1785/0120190166, 2020.

Bakun, W. and Scotti, O.: Regional intensity attenuation models for France and the estimation of magnitude and location of historical earthquakes, Geophys J Int, 164, 596–610, https://doi.org/10.1111/j.1365-246X.2005.02808.x, 2006.

Barszez, A.-M.: Aléa sismique du Bassin de Mons et vulnérabilité des bâtiments anciens – Analyse du risque sismique pour un quartier du centre historique de Mons., MSc-thesis, Faculté Polytechnique de Mons, Service d'Architecture et de Mines, 2005.

Bossu, R., Landès, M., Roussel, F., and Steed, R.: Felt Reports for Rapid Mapping of Global Earthquake Damage: The Doughnut Effect?, Seismological Research Letters, 89, 138–144, https://doi.org/10.1785/0220170129, _eprint: https://pubs.geoscienceworld.org/srl/article-pdf/89/1/138/4018549/srl-2017129.1.pdf, 2017.

Calais, E., Camelbeeck, T., Stein, S., Liu, M., and Craig, T.: A New Paradigm for Large Earthquakes in Stable Continental Plate Interiors, Geophysical Research Letters, 43, https://doi.org/10.1002/2016GL070815, 2016.

Cambier, R.: Les tremblements de terre de Ransart (mars, juin, juillet, 1911), Annales de la Société géologique de Belgique, 39, 97–101, 1911.

Camelbeeck, T.: Some Notes Concerning the Seismicity in Belgium — Magnitude Scale — Detection Capability of the Belgian Seismological Stations, in: Seismic Activity in Western Europe: with Particular Consideration to the Liège Earthquake of November 8, 1983, edited by Melchior, P. J., NATO ASI Series, pp. 99–108, Springer Netherlands, Dordrecht, https://doi.org/10.1007/978-94-009-5273-7_8, 1985a.

Camelbeeck, T.: Recent Seismicity in Hainaut — Scaling Laws from the Seismological Stations in Belgium and Luxemburg, in: Seismic activity in western Europe, pp. 109–126, Reidel, https://doi.org/10.1007/978-94-009-5273-7_9, 1985b.

Camelbeeck, T.: La séquence sismique dans la région de Dour de février à mai 1987, Bulletin de l'Académie Royale de Belgique, classe des sciences, 74, 96–116, https://doi.org/10.3406/barb.1988.57756, 1988.

Camelbeeck, T.: L'activité sismique actuelle (1985-1988) en Belgique. Comparaison avec les données de séismicité historique et instrumentale. Analyse séismotectonique, Annales de la Société géologique de Belgique, 112, 347–365, 1990.

Camelbeeck, T.: Mécanisme au foyer des tremblements de terre et contraintes tectoniques: le cas de la zone intraplaque belge, PhD Thesis, Université Catholique de Louvain, http://publi2-as.oma.be/record/1627/usage, 1993.

820 Camelbeeck, T., Snissaert, M., and Verbeiren, R.: The Belgian seismic network: present and future, Cahiers du centre européen de Géody-namique et de Séismologie, 1, 93–102, 1990.

Camelbeeck, T., van camp, M., Martin, H., Van de Putte, W., Bukasa, B., Castelein, S., Collin, F., Hendrickx, M., El Bouch, A., Petermans, T., Snissaert, M., Vanneste, K., and Verbeiren, R.: Les Effets en Belgique du Tremblement de Terre du 12 Juillet 2002 dans le Graben de la Roer, Ciel et Terre, 119, 2003.

825 Camelbeeck, T., de Viron, O., Van Camp, M., and Kusters, D.: Local stress sources in Western Europe lithosphere from geoid anomalies, Lithosphere, 5, 235–246, https://doi.org/10.1130/L238.1, 2013.

Camelbeeck, T., Alexandre, P., Sabbe, A., Knuts, E., Garcia Moreno, D., and Lecocq, T.: The impact of earthquake activity in Western Europe from the historical and architectural heritage records, in: Intraplate Earthquakes, Solid Earth Geophysics, pp. 198–230, Cambridge University Press, https://doi.org/10.1017/CBO9781139628921.009, 2014.

830 Camelbeeck, T., Knuts, E., Alexandre, P., Lecocq, T., and Van Noten, K.: The 23 February 1828 Belgian earthquake: a destructive moderate event typical of the seismic activity in Western Europe, Journal of Seismology, https://doi.org/10.1007/s10950-020-09977-6, 2021.

Capiau, H.: Secousse sismique ressentie le 15 janvier 1920 dans le Borinage., Annales de la Société géologique de Belgique, 43, 173–174, 1920.

Carriere, D.: Geocoder: Geocoder is a simple and consistent geocoding library., https://github.com/DenisCarriere/geocoder, 2021.

835 Cecić, I. and Musson, R.: Macroseismic Surveys in Theory and Practice, Natural Hazards, 31, 39–61, https://doi.org/10.1023/B:NHAZ.0000020255.00986.37, 2004.

Charlier, C.: Les séismes de la vallée de la Haine., Tech. rep., Publication provisoire, série S, Observatoire Royal de Belgique, 1949.

Charlier, C.: L'Effet d'écran du houiller dans la propagation des ondes séismiques et ses conséquences sur la forme des isoséistes., Académie royale de Belgique, Bulletin de la classe des Sciences, pp. 640–649, 1951.

840 Cornet, J.: Le tremblement de terre de Mons (12 avril 1911), Annales de la Société géologique de Belgique, 39, 39–97, 1911.

de Munck, E.: Les tremblements de terre d'Havré, Bulletin de la Société Belge de Géologie, de Paléontologie et d'Hydrologie, 1, 184–185, 1887.

Denieul, M.: Moment sismique et coda d'ondes crustales, PhD Thesis, Ecole Doctorale des Sciences de la Terre et de l'Environnement, EOST-IPGS de l'Université de Strasbourg, 2014.

845 Descamps, L.: Relations entre l'activité sismique dans le Hainaut et l'activité minière., Master's thesis, Faculté Polytechnique de Mons, University of Mons, 2009.

Dost, B. and Kraaijpoel, D.: The August 16, 2012 earthquake near Huizinge (Groningen)., Internal report of the KNMI, Royal Meteorological Institute of the Netherlands, 2013.

Drouet, S., Ameri, G., Le Dortz, K., Secanell, R., and Senfaute, G.: A probabilistic seismic hazard map for the metropolitan France, Bulletin
850 of Earthquake Engineering, 18, 1865–1898, https://doi.org/10.1007/s10518-020-00790-7, 2020.

Faber, S. and Bonjer, K.-P.: Phase Recognition and Interpretation at Regional Distances from the Liege Event of November 8, 1983, in: Seismic Activity in Western Europe: with Particular Consideration to the Liège Earthquake of November 8, 1983, edited by Melchior, P. J., NATO ASI Series, pp. 249–262, Springer Netherlands, Dordrecht, https://doi.org/10.1007/978-94-009-5273-7_20, 1985.

Garcia Moreno, D. and Camelbeeck, T.: Comparison of ground motions estimated from prediction equations and from observed
855 damage during the M=4.6 1983 Liège earthquake (Belgium), Natural Hazards and Earth System Sciences, 13, 1983–1997, https://doi.org/10.5194/nhess-13-1983-2013, 2013.

Gomberg, J. S., Shedlock, K. M., and Roecker, S. W.: The effect of S-wave arrival times on the accuracy of hypocenter estimation, Bulletin of the Seismological Society of America, 80, 1605–1628, 1990.

Grigoli, F., Cesca, S., Priolo, E., Rinaldi, A. P., Clinton, J. F., Stabile, T. A., Dost, B., Fernandez, M. G., Wiemer, S., and Dahm, T.: Current challenges in monitoring, discrimination, and management of induced seismicity related to underground industrial activities: A European perspective, Reviews of Geophysics, 55, 310–340, https://doi.org/https://doi.org/10.1002/2016RG000542, 2017.

Grünthal, G., Musson, R., Schartz, J., and Stucchi, M.: European Macroseismic Scale 1998, Cahiers du Centre Européen de Géodynamique et de Séismologie., Conseil de l'Europe, Luxembourg., 1998.

Hinzen, K.-G. and Oemisch, M.: Location and Magnitude from Seismic Intensity Data of Recent and Historic Earthquakes in the Northern Rhine Area, Central Europe, Bulletin of the Seismological Society of America, 91, 40–56, https://doi.org/10.1785/0120000036, 2001.

Hough, S. E. and Martin, S. S.: Which Earthquake Accounts Matter?, Seismological Research Letters, 92, 1069–1084, https://doi.org/10.1785/0220200366, 2021.

Hunter, J. D.: Matplotlib: A 2D Graphics Environment, Computing in Science & Engineering, 9, 90–95, https://doi.org/10.1109/MCSE.2007.55, 2007.

Jongmans, D. and Plumier, A.: Etude pilote du risque sismique sur une partie de la ville de Liège (4 km2), Internal report, Faculté des Sciences Appliquées, Université de Liège., 2000.

Knuts, E., Camelbeeck, T., and Alexandre, P.: The 3 December 1828 moderate earthquake at the border between Belgium and Germany, Journal of Seismology, 20, 419–437, https://doi.org/10.1007/s10950-015-9535-7, 2016.

Kárník, V.: Seismicity of the European Area: Part 2, Springer Netherlands, https://doi.org/10.1007/978-94-010-3078-6, 1971.

Köveslighety, R.: Seismischer Stärkegrad und Intensität der Beben, Gerlands Beiträge Geophysics, 8, 1907.

Lecocq, T., Rapagnani, G., Martin, H., Vos, F., Hendrickx, M., Van Camp, M., Vanneste, K., and Camelbeeck, T.: B-FEARS: The Belgian Felt Earthquake Alert and Report System, Cahiers du Centre Européen de Géodynamique et de Séismologie, 28, 2009.

Lecocq, T., Camelbeeck, T., Rapagnani, G., Bukasa, B., Castelein, S., Collin, F., Hendrickx, M., Martin, H., Vandercoilden, L., Van Camp, M., and Vanneste, K.: Trente ans de surveillance sismique en Belgique, Ciel et terre, 129, 105–109, 2013.

Leydecker, G., Grünthal, G., and Ahorner, L.: Der Gebirgsschlag vom 13. März 1989 bei Völkershausen in Thüringen im Kalibergbaugebiet des Werratals - Makroseismische Beobachtungen und Analysen, Geologisches Jahrbuch: Reihe E, Geophysik, 55, 5–24, 1998.

Leynaud, D., Jongmans, D., Teerlynck, H., and Camelbeeck, T.: Seismic hazard assessment in Belgium, Geologica Belgica, 3, 67–86, https://doi.org/10.20341/gb.2014.024, 2001.

Marlière, R.: Les tremblements de terre d'avril-mai 1949 dans la région de Mons, Bulletin de la Société belge de Géologie, de Paléontologie et d'Hydrologie, 60, 17–27, 1951.

Martin, C., Secanell, R., Combes, R., and Lignon, G.: Preliminary probabilistic seismic hazard assessement of France, London, 9-13 September, 2002.

McKinney, W.: Python for Data Analysis: Data Wrangling with Pandas, NumPy, and IPython, O'Reilly Media, Sebastopol, California, 2nd edition edn., 2017.

Nappi, R., Porfido, S., Paganini, E., Vezzoli, L., Ferrario, M. F., Gaudiosi, G., Alessio, G., and Michetti, A. M.: The 2017, MD = 4.0, Casamicciola Earthquake: ESI-07 Scale Evaluation and Implications for the Source Model, Geosciences, 11, 44, https://doi.org/10.3390/geosciences11020044, 2021.

Neefs, B., Van Noten, K., and Camelbeeck, T.: The complexity of modelling anisotropic intensity attenuation in Belgium, 37th General Assembly of the European Seismological Commission, Corfu, 19-24 September, 2021.

895 Nievas, C. I., Bommer, J. J., Crowley, H., van Elk, J., Ntinalexis, M., and Sangirardi, M.: A database of damaging small-to-medium magnitude earthquakes, Journal of Seismology, 24, 263–292, https://doi.org/10.1007/s10950-019-09897-0, 2020.

Oliphant, T. E.: A Guide to NumPy, Trelgol Publishing, 2006.

Phillips, D. W.: Macroseismic Effects of the Liège Earthquake with Particular Reference to Industrial Installations, in: Seismic Activity in Western Europe: with Particular Consideration to the Liège Earthquake of November 8, 1983, edited by Melchior, P. J., NATO ASI Series,
900 pp. 369–384, Springer Netherlands, Dordrecht, https://doi.org/10.1007/978-94-009-5273-7_30, 1985.

Plumier, A.: Les effets sur les constructions. Les réparations., in: Le séisme de Liège et ses implications pratiques, vol. 4 of *Annales des travaux publics de Belgique*, pp. 346–353, Breesch, L., Camelbeeck, T., De Becker, M., Gurpinar, A., Monjoie, A., Plumier, A. and Van Gils, J.M., 1985.

Plumier, A.: Risque sismique sur une partie de la ville de Liège, in: Proceedings du colloque « Evaluation et prévention du risque sismique
905 en Wallonie » organisé par la Région Wallonne les 16 et 17 Octobre 2007, pp. 47–56, Namur, Belgique, 2007.

Provost, L. and Scotti, O.: QUake-MD: Open-Source Code to Quantify Uncertainties in Magnitude–Depth Estimates of Earthquakes from Macroseismic Intensities, Seismological Research Letters, 91, 2520–2530, https://doi.org/10.1785/0220200064, 2020.

QGIS Development Team: QGIS Geographic Information System, Open Source Geospatial Foundation. Last Access: 10 March 2021, http://qgis.osgeo.org, 2021.

910 Sbarra, P., Burrato, P., Tosi, P., Vannoli, P., De Rubeis, V., and Valensise, G.: Inferring the depth of pre-instrumental earthquakes from macroseismic intensity data: a case-history from Northern Italy, Scientific Reports, 9, 15 583, https://doi.org/10.1038/s41598-019-51966-4, 2019.

Sira, C.: Macroseismic Intervention Group: The Necessary Field Observation, pp. 395–408, Springer International Publishing, Cham, https://doi.org/10.1007/978-3-319-16964-4_16, 2015.

915 Sira, C., Schlupp, A., Dretzen, R., Maufroy, E., Provost, L., Bertrand, E., Beck, E., and Schaming, M.: Rapport macrosismique n°4. Séisme du Teil (Ardèche). 11 novembre 2019 à 11h52 locale. Magnitude 5,2 ML(RENASS). Intensité communale max VII-VIII (EMS98), report, BCSF-RENASS, http://www.franceseisme.fr/donnees/intensites/2019/191111_1052/Rapport%20macrosismique%20V4%20BCSF-RENASS%20Sei2019-11-11-RP.pdf, 2019.

Somville, O.: Les tremblements de terre en Belgique, Edt Imprimerie Duculot (Gembloux), Observatoire royal de Belgique, 1936.

920 Sponheuer, W.: Untersuchungen Zur Seismizität von Deutschland, Veröffentlichungen des Instituts für Bodenmechanik und Erdbeben-forschung in Jena, 72, 23–52, 1962.

State Archives of Belgium: Last Access: 10 March 2021., http://arch.arch.be, 2021.

Stromeyer, D. and Grünthal, G.: Attenuation Relationship of Macroseismic Intensities in Central Europe, Bulletin of the Seismological Society of America, 99, 554–565, https://doi.org/10.1785/0120080011, 2009.

925 Stromeyer, D., Grünthal, G., and Wahlström, R.: Chi-square regression for seismic strength parameter relations, and their uncertainties, with applications to an Mw based earthquake catalogue for central, northern and northwestern Europe, Journal of Seismology, 8, 143–153, https://doi.org/10.1023/B:JOSE.0000009503.80673.51, 2004.

Troch, K.: Une vulnérabilité délibérément acceptée par les pouvoirs publics ? Extraction du charbon et inondations dans la vallée de la Haine, 1880-1940, VertigO - la revue électronique en sciences de l'environnement, 16, https://doi.org/10.4000/vertigo.17998, 2016.

930 Troch, K.: Ne pas grever l'avenir au bénéfice du présent : Une histoire environnementale de l'extraction du charbon de la fin du 18e siècle à l'Entre-deux-guerres : un développement non soutenable. : L'exemple du Couchant de Mons et du Valenciennois, PhD Thesis, Université Charles de Gaulle - Lille III ; Université de Namur, 2018a.

Troch, K.: Reforming Mineral Ownership and Ensuring Surface Owners' Rights: The Gosselies Disaster, Global Environment, 11, 319–345, https://doi.org/10.3197/ge.2018.110206, 2018b.

935 Van Gils, J.-M.: Les séismes des 15 et 21 décembre 1965 et du 16 janvier 1966., Ciel et Terre, 82, 243–267, 1966.

Van Gils, J.-M. and Zaczek, Y.: La séismicité de la Belgique et son application en génie parasismique, Annales des Travaux Publics de Belgique, 6, 502–539, 1978.

Van Noten, K., Lecocq, T., Shah, A. K., and Camelbeeck, T.: Seismotectonic significance of the 2008–2010 Walloon Brabant seismic swarm in the Brabant Massif, Belgium, Tectonophysics, 656, 20–38, https://doi.org/https://doi.org/10.1016/j.tecto.2015.05.026, 2015.

940 Van Noten, K., Lecocq, T., Sira, C., Hinzen, K.-G., and Camelbeeck, T.: Path and site effects deduced from merged transfrontier internet macroseismic data of two recent M4 earthquakes in northwest Europe using a grid cell approach, Solid Earth, 8, 453–477, https://doi.org/10.5194/se-8-453-2017, 2017.

Vanneste, K., Vleminckx, B., Verbeeck, K., and Camelbeeck, T.: Development of seismic hazard maps for Belgium, pp. 61–68, Seismic Hazard Harmonization in Europe (SHARE): DGEB-Workshop, Print Office Schumacher, Herzogenrath, 2014.

945 Virtanen, P., Gommers, R., Oliphant, T. E., Haberland, M., Reddy, T., Cournapeau, D., Burovski, E., Peterson, P., Weckesser, W., Bright, J., van der Walt, S. J., Brett, M., Wilson, J., Millman, K. J., Mayorov, N., Nelson, A. R. J., Jones, E., Kern, R., Larson, E., Carey, C. J., Polat, I., Feng, Y., Moore, E. W., VanderPlas, J., Laxalde, D., Perktold, J., Cimrman, R., Henriksen, I., Quintero, E. A., Harris, C. R., Archibald, A. M., Ribeiro, A. H., Pedregosa, F., and van Mulbregt, P.: SciPy 1.0: fundamental algorithms for scientific computing in Python, Nature Methods, 17, 261–272, https://doi.org/10.1038/s41592-019-0686-2, 2020.

950 Woessner, J., Laurentiu, D., Giardini, D., Crowley, H., Cotton, F., Grünthal, G., Valensise, G., Arvidsson, R., Basili, R., Demircioglu, M. B., Hiemer, S., Meletti, C., Musson, R. W., Rovida, A. N., Sesetyan, K., Stucchi, M., and The SHARE Consortium: The 2013 European Seismic Hazard Model: key components and results, Bulletin of Earthquake Engineering, 13, 3553–3596, https://doi.org/10.1007/s10518-015-9795-1, 2015.